JVI Journals.ASM.org

Biology of Zika Virus Infection in Human Skin Cells

Rodolphe Hamel,[a] Ophélie Dejarnac,[b] Sineewanlaya Wichit,[a] Peeraya Ekchariyawat,[a] Aymeric Neyret,[c] Natthanej Luplertlop,[d] Manuel Perera-Lecoin,[a] Pornapat Surasombatpattana,[e] Loïc Talignani,[a] Frédéric Thomas,[a] Van-Mai Cao-Lormeau,[f] Valérie Choumet,[g] Laurence Briant,[c] Philippe Desprès,[h] Ali Amara,[b] Hans Yssel,[i] Dorothée Missé[a]

Laboratoire MIVEGEC, UMR 224 IRD/CNRS/UM, Montpellier, France[a]; INSERM, U944, Laboratoire de Pathologie et Virologie Moléculaire, Paris, France[b]; Centre d'Étude d'Agents Pathogènes et Biotechnologies pour la Santé, CNRS-UMR 5236/UM, Montpellier, France[c]; Department of Microbiology and Immunology, Faculty of Tropical Medicine, Mahidol University, Bangkok, Thailand[d]; Pathology Department, Prince of Songkla University, Songkla, Thailand[e]; Institut Louis Malardé, Papeete, Tahiti, French Polynesia[f]; Environment and Infectious Risks Unit, Institut Pasteur, Paris, France[g]; Département Infections et Epidémiologie, Institut Pasteur, Paris, France, and UMR PIMIT (I2T Team), Université de La Réunion, INSERM U1187, CNRS 9192, IRD 249, GIP-CYROI, Saint Clotilde, La Réunion, France[h]; Centre d'Immunologie et des Maladies Infectieuses, INSERM, U1135, Sorbonne Universités, UPMC, APHP Hôpital Pitié-Salpêtrière, Paris, France[i]

ABSTRACT

Zika virus (ZIKV) is an emerging arbovirus of the *Flaviviridae* family, which includes dengue, West Nile, yellow fever, and Japanese encephalitis viruses, that causes a mosquito-borne disease transmitted by the *Aedes* genus, with recent outbreaks in the South Pacific. Here we examine the importance of human skin in the entry of ZIKV and its contribution to the induction of antiviral immune responses. We show that human dermal fibroblasts, epidermal keratinocytes, and immature dendritic cells are permissive to the most recent ZIKV isolate, responsible for the epidemic in French Polynesia. Several entry and/or adhesion factors, including DC-SIGN, AXL, Tyro3, and, to a lesser extent, TIM-1, permitted ZIKV entry, with a major role for the TAM receptor AXL. The ZIKV permissiveness of human skin fibroblasts was confirmed by the use of a neutralizing antibody and specific RNA silencing. ZIKV induced the transcription of Toll-like receptor 3 (TLR3), RIG-I, and MDA5, as well as several interferon-stimulated genes, including OAS2, ISG15, and MX1, characterized by strongly enhanced beta interferon gene expression. ZIKV was found to be sensitive to the antiviral effects of both type I and type II interferons. Finally, infection of skin fibroblasts resulted in the formation of autophagosomes, whose presence was associated with enhanced viral replication, as shown by the use of Torin 1, a chemical inducer of autophagy, and the specific autophagy inhibitor 3-methyladenine. The results presented herein permit us to gain further insight into the biology of ZIKV and to devise strategies aiming to interfere with the pathology caused by this emerging flavivirus.

IMPORTANCE

Zika virus (ZIKV) is an arbovirus belonging to the *Flaviviridae* family. Vector-mediated transmission of ZIKV is initiated when a blood-feeding female *Aedes* mosquito injects the virus into the skin of its mammalian host, followed by infection of permissive cells via specific receptors. Indeed, skin immune cells, including dermal fibroblasts, epidermal keratinocytes, and immature dendritic cells, were all found to be permissive to ZIKV infection. The results also show a major role for the phosphatidylserine receptor AXL as a ZIKV entry receptor and for cellular autophagy in enhancing ZIKV replication in permissive cells. ZIKV replication leads to activation of an antiviral innate immune response and the production of type I interferons in infected cells. Taken together, these results provide the first general insights into the interaction between ZIKV and its mammalian host.

Zika virus (ZIKV) is a little-known emerging mosquito-borne flavivirus, of the *Flaviviridae* family, that is closely related to the Spondweni serocomplex. Like other members of the *Flavivirus* genus, ZIKV contains a positive, single-stranded genomic RNA encoding a polyprotein that is processed into three structural proteins, i.e., the capsid (C), the precursor of membrane (prM), and the envelope (E), and seven nonstructural proteins, i.e., NS1 to NS5 (1). Virus replication occurs in the cellular cytoplasm.

Epidemiological studies point to a widespread distribution of ZIKV in the northern half of the African continent, as well as in many countries in Southeast Asia, including Malaysia, India, the Philippines, Thailand, Vietnam, Indonesia, and Pakistan (2–9). Many different *Aedes* species mosquitoes can account for the transmission of ZIKV, including *Aedes aegypti* (10, 11), which at present is considered to be the main vector of the virus in South and Southeast Asia (11, 12). The first human ZIKV infection was reported in Uganda in 1964 (2, 3, 5, 13), and the virus was later isolated from humans in Southeast Asia (8, 14–16). Despite this broad geographical distribution, human ZIKV infections remained sporadic and limited to small-scale epidemics for decades, until 2007, when a large epidemic was reported on Yap Island, a territory of the Federated States of Micronesia, with nearly 75% of the population being infected with the virus (17).

Received 10 February 2015 **Accepted** 8 June 2015

Accepted manuscript posted online 17 June 2015

Citation Hamel R, Dejarnac O, Wichit S, Ekchariyawat P, Neyret A, Luplertlop N, Perera-Lecoin M, Surasombatpattana P, Talignani L, Thomas F, Cao-Lormeau V-M, Choumet V, Briant L, Desprès P, Amara A, Yssel H, Missé D. 2015. Biology of Zika virus infection in human skin cells. J Virol 89:8880–8896. doi:10.1128/JVI.00354-15.

Editor: M. S. Diamond

Address correspondence to Dorothée Missé, dorothee.misse@ird.fr.

O.D. and S.W. contributed equally to this article.

Supplemental material for this article may be found at http://dx.doi.org/10.1128/JVI.00354-15.

doi:10.1128/JVI.00354-15

Moreover, an outbreak of a syndrome due to Zika fever has been reported in French Polynesia, in addition to several cases of ZIKV infection in New Caledonia, Easter Island, and the Cook Islands, indicating a rapid spread of the virus in the Pacific (18). Also, two imported cases of ZIKV infection of travelers, from Indonesia and the Cook Islands to Australia, and two cases imported from Thailand, to Europe and Canada, were described recently (19–22), emphasizing the capacity of ZIKV to spread to areas where it is not endemic but where the proper mosquito vector might be present. The largest outbreak of ZIKV ever reported was characterized by fever, rash, arthralgia, and conjunctivitis in infected individuals. Moreover, during the recent outbreak in French Polynesia, ZIKV infection-related neurological disorders were also described, and the incidence of Guillain-Barré syndrome unexpectedly increased 20-fold (23). In the absence of monkeys in French Polynesia, it is likely that humans served as primary amplification hosts for ZIKV.

Because ZIKV has received far less attention than other emerging arboviruses, such as yellow fever, dengue (DENV), West Nile (WNV), Japanese encephalitis, and Chikungunya viruses, the pathogenesis of ZIKV infection still remains poorly understood. Mosquito-mediated transmission of ZIKV is initiated when a blood-feeding female *Aedes* mosquito injects the virus into human skin, followed by infection of permissive cells (reviewed in reference 24). However, no information is available either on the nature of the skin cells that are permissive to infection with ZIKV or on the entry receptor used by this flavivirus. Moreover, the mechanisms of ZIKV infection and the signaling pathways and antiviral immune response of the host elicited by this virus remain to be determined. In the present study, we describe the entry receptors and cellular targets of the most recent ZIKV isolate, responsible for the recent epidemic in French Polynesia, to provide general insights into the interaction between this virus and its human host.

MATERIALS AND METHODS

Ethics statement. The study was approved by the IRD ethics committee (registration number AC-2013-1754), and all donors gave written informed consent.

Cells, viruses, and reagents. *A. albopictus* C6/36 cells, used for propagation of the ZIKV strain, were grown in Dulbecco's modified Eagle's medium (DMEM; Invitrogen, Cergy Pontoise, France) supplemented with 10% fetal calf serum (FCS; Lonza, Basel, Switzerland) at 28°C, as previously described (25). Primary human dermal fibroblasts were obtained from neonatal foreskins and cultured at 37°C and 5% CO_2 in fibroblast basal medium 2 supplemented with FGM-2 supplements and growth factors (all purchased from Lonza). The HFF-1 skin fibroblast cell line and HEK293T, A549, and Vero cells were maintained in DMEM supplemented with 10% FCS. HEK293T cells stably expressing DC-SIGN, TIM-1, TIM-4, AXL, or Tyro3 have been reported previously (26). Primary human epidermal keratinocytes were obtained from neonatal foreskins (Lonza, Basel, Switzerland) and cultured at 37°C and 5% CO_2 in keratinocyte basal medium 2 (Lonza, Basel, Switzerland) supplemented with KGM-2 supplements and growth factors (Lonza, Basel, Switzerland). The low-passage-number PF-25013-18 strain of ZIKV (obtained via V. M. Cao-Lormeau and D. Musso, Institut Louis Malardé [ILM], Tahiti Island, French Polynesia), isolated from a viremic patient in French Polynesia in 2013, was used in the current study and was grown in *A. albopictus* C6/36 mosquito cells. The DENV-2 Jamaica/N.1409 strain (GenBank accession no. M20558.1) was propagated in AP61 cell monolayers after having undergone limited cell passages. Recombinant human alpha interferon (IFN-α), IFN-β, and IFN-γ and the Torin 1 autophagy inducer were purchased from R&D Systems (Lille, France). The autophagy inhibitor 3-methyladenine (3-MA) was purchased from Sigma.

Dendritic cell generation. Human peripheral blood mononuclear cells were isolated from healthy donors by density centrifugation over Ficoll-Paque Plus (Amersham Biosciences, France). Monocytes were negatively selected with magnetic beads coated with a mixture of antibodies (Abs; Miltenyi Biotec, France) and seeded at 10^6 cells/ml in RPMI 1640 supplemented with 10% FCS, 1% penicillin-streptomycin, 50 ng/ml recombinant human interleukin-4 (PeproTech, France), and 100 ng/ml recombinant human granulocyte-macrophage colony-stimulating factor (PeproTech, France) for 7 days.

ZIKV infection of cells. For infection, cells were seeded in culture plates at 4×10^4 cells per cm^2. The cells were then rinsed once with phosphate-buffered saline (PBS), and ZIKV diluted to the desired multiplicity of infection (MOI) was added to the cells. The cells were incubated for 2 h at 37°C with gentle agitation every 30 min. Next, the inoculum was removed and the cells were washed twice with PBS. Culture medium was added to each well, and the cells were incubated at 37°C and 5% CO_2 for the duration of the experiment. As a control, fibroblasts were incubated with the culture supernatant from uninfected C6/36 cells, referred to in the present study as mock-infected cells.

ZIKV infection of human skin biopsy specimens. Fresh, sterile human skin biopsy specimens of 88 mm were obtained from three adult healthy donors (age range, 38 to 43 years) following abdominoplastic surgery. The skin explants were cultured as described by Limon-Flores et al. (27). For infection, 10^6 PFU in a final volume of 50 μl DMEM was injected into each biopsy specimen. As a control, skin biopsy specimens were injected with culture supernatant from uninfected C6/36 cells in a final volume of 50 μl DMEM. At different time points, the biopsy specimens were harvested and soaked with enzymes that degrade the extracellular matrix by using a whole-skin dissociation kit (Miltenyi Biotec, Paris, France). In the second step, single cells were freed from the extracellular matrix by using gentleMACS Dissociator (Miltenyi Biotec, Paris, France), and cells were lysed with Tri reagent (Sigma, Saint Quentin Fallavier, France) for reverse transcription-PCR (RT-PCR) analysis. For histological analysis, biopsy specimens were fixed in neutral buffered formalin and embedded in paraffin. Tissue sections (3 to 5 μm) were stained with hematoxylin-eosin, placed on slides, and digitalized with a Nanozoomer scanner (Hamamatsu, Massy, France) with a 20× objective.

ZIKV real-time RT-PCR. Total RNA was extracted from human fibroblasts by using Tri reagent (Sigma, Saint Quentin Fallavier, France) according to the manufacturer's protocol. The RNA pellet was resuspended in 30 μl of RNase-free distilled water and stored at 80°C. One microgram of RNA was used for reverse transcription using Moloney murine leukemia virus (M-MLV) reverse transcriptase (Promega, Charbonnieres, France) according to the manufacturer's instructions. Maxima probe/ROX qPCR master mix (Fermentas, Saint Remy les Chevreuses, France) was used for all quantitative PCRs (qPCRs). Each 25-μl reaction mixture contained 500 nM forward primer, 500 nM reverse primer, 250 nM specific probe, and 1× (final concentration) Maxima probe/ROX qPCR master mix. The primer and probe sequences targeting ZIKV have already been described (28). Amplification in an Applied Biosystems 7300 real-time PCR system involved activation at 95°C for 10 min followed by 40 amplification cycles of 95°C for 15 s, 60°C for 15 s, and 72°C for 30 s. Real-time data were analyzed using SDS software from Applied Biosystems. Viral RNA was quantified by comparing each sample's threshold cycle (C_T) value with a ZIKV RNA standard curve, which was obtained as follows. First, total viral RNA from the cell culture was purified using a QIAamp viral RNA kit (Qiagen, Courtaboeuf, France) following the manufacturer's protocol. A standard RT-PCR was then carried out by using primers containing the T7 promoter sequence (T7-ZIKV_F, TAATACGACTCACTATAGGGTTGGTCATGATACTGCTGATTGC; and ZIKV_R, CCTTCCACAAAGTCCCTATTGC). The PCR product was used to generate ZIKV RNA fragments by *in vitro* transcription using a MAXIscript kit (Ambion, Austin, TX). RNA was then purified by ethanol precipitation, and the

RNA strands generated were determined by spectrophotometry and converted to numbers of molecular copies by using the following formula: number of *y* molecules per microliter = [(*x* grams per microliter of RNA)/(transcript length in base pairs × 340)] × 6.02 × 10^{23}. RNA standards containing RNA copies were used to construct a standard curve.

Real-time PCR analysis. cDNA was synthesized using 2 μg RNA and an M-MLV reverse transcription kit (Promega, Charbonière, France) following the manufacturer's protocol. Gene expression was quantified using real-time PCR with an Applied Biosystems 7300 real-time PCR system. Real-time PCR was performed using 2 μl of cDNA with specific primers targeting the genes of interest (see Table S1 in the supplemental material) and 10 μl of Maxima Sybr/ROX qPCR master mix (Fermentas, Saint Remy les Chevreuses, France) in a final reaction volume of 20 μl. The cycling conditions were 45 cycles of 95°C for 15 s, 60°C for 15 s, and 72°C for 30 s. mRNA expression (fold induction) was quantified by calculating the $2^{-\Delta\Delta CT}$ value, with glyceraldehyde-3-phosphate dehydrogenase (GAPDH) mRNA as an endogenous control.

RT2 Profiler PCR array. Total RNA was extracted from primary human skin fibroblasts by using Tri reagent (Sigma, Saint Quentin Fallavier, France) according to the manufacturer's instructions. The concentrations of all RNA samples were assessed using a NanoDrop spectrophotometer (NanoDrop Technologies, Wilmington, DE). The same amount of total RNA (400 ng) from each sample was subjected to a cDNA synthesis reaction by using an RT2 First Strand kit (Qiagen, Valencia, CA). The resulting cDNA reaction mixture (20 μl per sample) was diluted in 91 μl of nuclease-free H_2O (Qiagen). The diluted cDNA (102 μl) was mixed with 1,248 μl of H_2O plus 1,350 μl of 2× RT^2 SYBR green RT^2 master mix. The cocktail was dispensed at 10 μl per well into a 384-well RT2 Profiler PCR array plate for profiling of a total of 84 genes, as described in the manufacturer's handbook (PAHS-122Z; SABiosciences, Frederick, MD). Five housekeeping genes (encoding ACTB, B2M, GAPDH, HPRT1, and RPL13A) were used as internal controls. DNA amplification was carried out with a Roche LightCycler 480 real-time cycler, using the following cycling program: 95°C for 10 min followed by 40 cycles of 95°C for 15 s and 60°C for 1 min, followed by a melting curve acquisition step. The resulting threshold cycle values for the plate were exported to a blank Excel worksheet. An automatic datasheet for analysis was downloaded from the SABiosciences Web portal. The fold changes of gene expression were calculated in comparison to the values for the controls, as follows: fold change = inline eq$2^{-(\Delta C_T}$ experiment $- \Delta C_T$ control), where $\Delta C_T = C_T$(gene of interest) $- C_T$(housekeeping gene). The average of reverse transcription control values and positive PCR control C_T values was used to normalize gene expression and determine fold changes between groups. To evaluate gene expression, we selected a fold change threshold of at least 2-fold up- or downregulation compared with the level in mock-infected cells. Gene regulation was considered statistically significant at a 95% confidence level ($P < 0.05$). The confidence level was determined from data obtained in triplicate for each sample. Statistical analysis was performed using the RT^2 profiler RT-PCR array data analysis software, version 3.5.

Immunolabeling. Twenty-four and 48 h following infection of fibroblasts, ZIKV-infected and mock-infected cells were fixed with 3.7% paraformaldehyde in PBS for 1 h at room temperature. Slides were blocked by incubation in 10% FCS and 0.3% Triton X-100 for 30 min and then incubated for 2 h at 37°C with the monoclonal antibody (MAb) 4G2, which is directed against the flavivirus envelope protein. Cells were washed with PBS and incubated for 60 min at room temperature with fluorescein isothiocyanate (FITC)-conjugated anti-mouse IgG. Hoechst 33258 dye was used to stain the nucleus. Preparations were examined with a Zeiss Apotome/Axioimager device. Autophagy was monitored after fixation of the cells in a 3.7% paraformaldehyde-PBS solution for 10 min at room temperature, permeabilization, and labeling with anti-LC3 MAbs (Sigma). Coverslips were analyzed by epifluorescence microscopy using a Leica microscope.

Electron microscopy. Primary human fibroblasts were exposed to ZIKV at an MOI of 10, cultured at 5% CO_2 for 72 h, collected, washed twice with PBS, and fixed for 1 h at 4°C in a solution containing 2.5% glutaraldehyde in 0.1 M cacodylate buffer, pH 7.4. Cells were then rinsed three times in cacodylate buffer and postfixed for 1 h with 1% OsO_4 (Electron Microscopy Sciences Inc.). After an additional washing, the cells were incubated for 30 min in 0.5% tannic acid (Merck). Dehydration was obtained by using a graded series of ethanol solutions (from 25 to 100%) before embedding the samples in Epok resin at 60°C for 48 h (Electron Microscopy Sciences Inc.). Ultrathin sections were cut with a Reichert Ultracut microtome (Leica) and then examined under a Hitachi H7100 transmission electron microscope at 75 kV.

ZIKV plaque assay. Four different 10-fold dilutions of purified virus were spread onto monolayers of Vero cells at 37°C for 2 h to initiate binding to cells. A mix of nutriment solution with agar (Lonza) was then added. The cells were maintained at 37°C for 6 days before the plaque assay. For plaque counting, the cells were incubated with 3.7% formaldehyde and 0.1% crystal violet in 20% ethanol. This experiment was repeated three times.

Western blotting. Cells were lysed on ice in RIPA buffer (150 mM NaCl, 5 mM β-mercaptoethanol, 1% NP-40, 0.1% sodium dodecyl sulfate, 50 mM Tris-HCl, pH 8) supplemented with Complete protease inhibitor cocktail solution (Sigma). The protein concentration was determined by bicinchoninic acid (BCA) assay (Thermo Scientific, Saint Herblain, France). Equal amounts of proteins were mixed with Laemmli sample buffer, subjected to SDS-PAGE, and electrotransferred onto a nitrocellulose membrane. The membrane was blocked with PBS-0.05% Tween 20 containing 5% skim milk, incubated overnight at 4°C with anti-MX1 as the primary antibody, washed three times with PBS-Tween, and subsequently incubated for 1 h at room temperature with horseradish peroxidase-coupled secondary antibodies in PBS-Tween containing 1% skim milk. The membrane was washed three times, and proteins were detected by chemiluminescence using a SuperSignal West Pico chemiluminescent substrate kit (Thermo Scientific). The immunoblot was then stripped and reblotted with an anti-α-tubulin Ab to ensure that equivalent levels of protein were loaded in each lane.

Flow cytometry analysis. Flow cytometry analysis was performed as previously described (26). ZIKV infection was detected using the anti-4G2 MAb.

Inhibition of infection. Cells were incubated for 30 min prior to infection with medium containing the indicated quantities of goat anti-TIM and/or anti-AXL polyclonal antibody. Identical concentrations of purified normal goat IgG were used as a control. Cells were then infected with ZIKV or DENV for 3 h in the presence of inhibitors, washed, and incubated with culture medium. Infection was quantified by flow cytometry.

RNA interference. Cells were transiently transfected with a 10 nM final concentration of small interfering RNAs (siRNAs) (26) by using the Lipofectamine RNAiMax protocol (Life Technologies). After 48 h, cells were infected at the indicated MOI, and percentages of infected cells at 24 h postinfection were quantified by flow cytometry. For pattern recognition receptor (PRR) signaling pathways, a 50 nM final concentration of siRNAs was used. The following pools of siRNAs (ON-TARGETplus SMARTpool) used in this study were from Dharmacon: siRNA pools for TIM-1 (L-019856-00), AXL (L-003104-00), Toll-like receptor 3 (TLR3) (L-007745-00), TLR7 (L004714-00), RIG-I (L-012511-00), and MDA5 (L-013041-00). A nontargeting pool (NT) was used as a negative control.

RESULTS

Human skin cells are permissive for ZIKV infection and replication. Given the capacity of mosquitoes to inoculate ZIKV into the human skin during the blood-feeding process, the potential target cells for infection with this virus are likely to be localized to the epidermis and dermis, which also constitute the first line of defense. We first determined the ZIKV susceptibility of skin fibroblasts, which have been recognized as a permissive target for var-

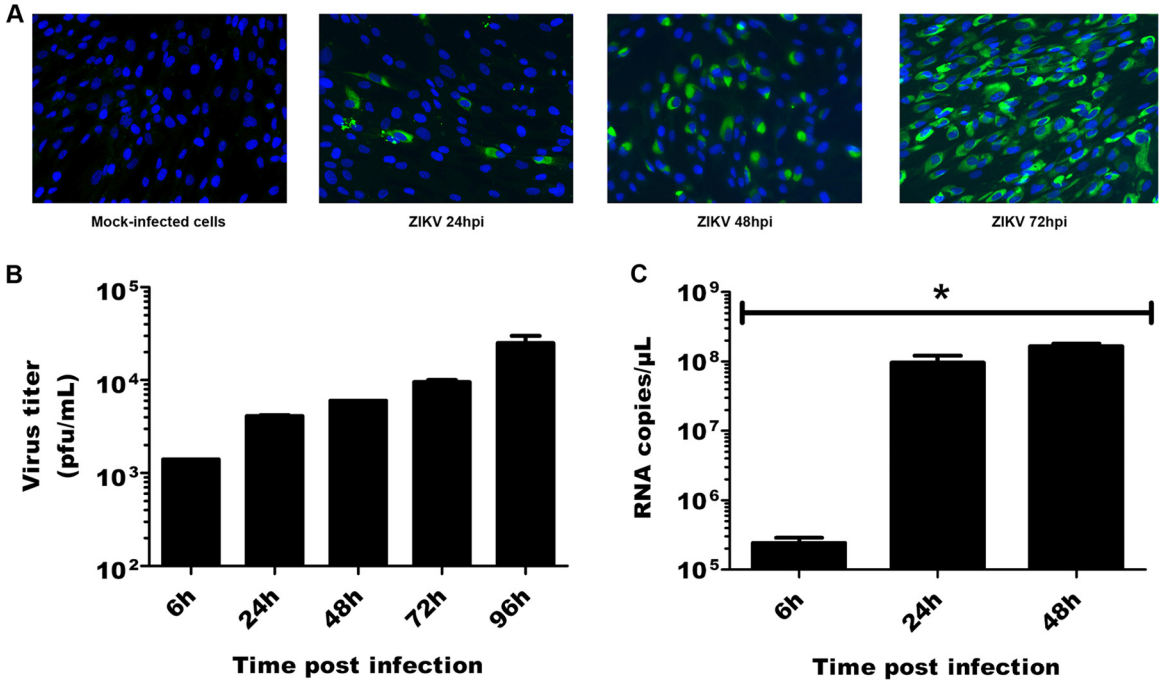

FIG 1 Primary human fibroblasts are susceptible to ZIKV. (A) Primary fibroblasts infected with ZIKV (MOI = 1) and mock-infected cells were analyzed at different times postinfection for the presence of the viral envelope protein by immunofluorescence with the 4G2 MAb and an FITC-conjugated anti-mouse IgG. (B) Viral replication was determined by plaque assay of culture supernatants of ZIKV-infected cells. (C) Expression of viral RNA was determined by real-time RT-PCR. Data are representative of three independent experiments, each performed in duplicate (error bars represent standard errors of the means [SEM]). The Wilcox-Mann-Whitney test was employed to analyze the differences between sets of data. *, $P < 0.05$.

ious arboviruses. Cells were infected *in vitro* with ZIKV, and the presence of viral envelope antigens was evaluated by immunofluorescence at different hours postinfection (hpi). No staining was observed in mock-infected cells or cells stained with an isotype control antibody (Fig. 1A). In contrast, as soon as 24 hpi, the viral envelope protein was detected in several cells, whereas at 72 hpi, 100% of the infected cells expressed ZIKV (Fig. 1A). Next, we evaluated the ability of these cells to produce viral progeny *in vitro* by determining viral titers in the supernatants of ZIKV-infected primary human skin fibroblasts, using a standard plaque assay. The results show a gradual increase in the production of viral particles over time, indicating active viral replication in the infected cells (Fig. 1B). Intracellular viral RNA was also quantified by real-time PCR at different time points postinfection. ZIKV RNA was detected in fibroblasts challenged with the virus but not in mock-infected cells, as shown in Fig. 1C. Viral RNA copy numbers could be determined as soon as 6 hpi and increased during the course of infection. The amounts of viral transcripts were markedly high and could reach 10^8 RNA copies/μl in cells infected with ZIKV and maintained in culture for 24 to 48 h.

Next, given the observation that the epidermal layer is comprised mainly of keratinocytes, we hypothesized that the latter cells could also be a target for ZIKV. Primary human epidermal keratinocytes obtained from neonatal foreskin were infected with ZIKV, and intracellular viral RNA was quantified by quantitative PCR at different time points postinfection. As shown in Fig. 2A, ZIKV mRNA was detected in keratinocytes challenged with ZIKV, but it was not detected in mock-infected cells. Viral RNA was found to increase over time and could be detected as soon as 6 hpi, with a maximal amount of 10^5 viral copies per ml, at both 48 and 72 hpi. The capacity of ZIKV to replicate *ex vivo* in human skin cells was also studied. Infection of human skin explants with ZIKV resulted in a gradual increase in the viral copy number, with maximal levels at 5 days postinfection (dpi), pointing to a process of active viral replication (Fig. 2B). Histological analysis of mock-infected human skin explants showed all aspects of normal, healthy skin, with a stratified epidermal layer containing basal keratinocytes and differentiated layers consisting of stratum granulosum and stratum corneum (Fig. 2C). In contrast, ZIKV-infected keratinocytes in human skin explants at 5 dpi showed the appearance of cytoplasmic vacuolation as well as the presence of pyknotic nuclei, which was, however, not generalized throughout the epidermis but limited to the stratum granulosum (Fig. 2D). Moreover, ZIKV infection induced the sporadic formation of edema, which was also limited to this subcorneal layer (Fig. 2E).

Immature dendritic cells have been reported to be permissive for DENV infection, and as such, they are recognized as an important target for propagation of this virus in the human skin. ZIKV infection was therefore also investigated on this cell type, using DENV as a control, by analyzing the intracellular presence of the viral envelope protein by flow cytometry. Our results show that about 50% of human *in vitro*-generated immature dendritic cells challenged with ZIKV at an MOI of 0.5 for 24 hpi expressed the viral envelope (Fig. 3). This percentage is identical to that for cells infected with DENV under the same experimental conditions. These results indicate that immature dendritic cells are also permissive to infection by this member of the flavivirus family.

DC-SIGN, TIM, and TAM receptors are involved in ZIKV infection. Several receptors, including DC-SIGN and certain TIM and TAM proteins, two members of the phosphatidylserine recep-

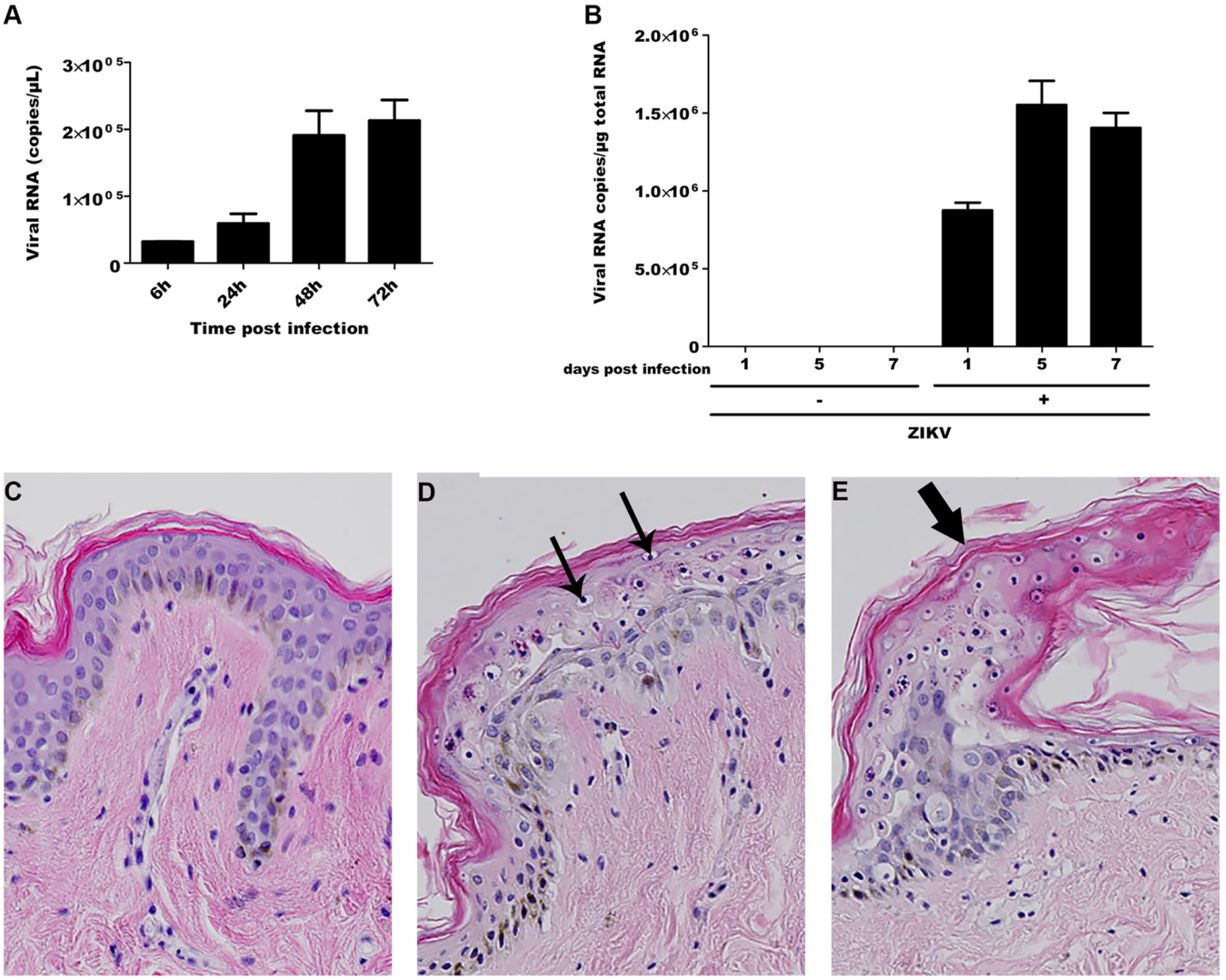

FIG 2 ZIKV infects human keratinocytes and induces morphological changes in human skin biopsy specimens. Primary human keratinocytes (A) and human skin biopsy specimens (B) were infected with ZIKV (MOI of 1 and 10^6 PFU, respectively), and expression of viral RNA was determined at different time points by real-time RT-PCR. Data are representative of three independent experiments, each performed in duplicate (error bars represent SEM). The Wilcox-Mann-Whitney test was employed to analyze the differences between sets of data. *, $P < 0.05$. (C to E) Microscopic observation of mock (C)- or ZIKV (D and E)-infected human skin biopsy specimens. Small arrows indicate keratinocyte cytoplasmic vacuolation. The large arrow indicates a superficial subcorneal edema, and also cytoplasmic vacuolation. Magnification, ×20. Data are representative of two independent experiments.

tor family, have been reported to facilitate viral entry of DENV (reviewed in reference 29). To determine whether these receptors are also involved in ZIKV entry, a series of HEK293T cell transfectants, expressing DC-SIGN, TIM-1, TIM-4, or a TAM family member (AXL or Tyro3) in a stable manner, were exposed to the virus. The expression levels of these receptors are shown in Fig. 4A. The parental, nontransfected HEK293T cells were not susceptible to ZIKV infection, as shown by the absence of ZIKV antigen detection (Fig. 4B). The expression of either DC-SIGN or AXL strongly enhanced viral infection already at an MOI of 0.1, resulting in about 50% ZIKV-infected cells. Tyro3-expressing HEK293T cells were also highly permissive for ZIKV, with nearly 70% of the cells infected with the virus at 24 hpi. In contrast, the expression of TIM-1 or TIM-4 had only modest or marginal effects on ZIKV entry (Fig. 4B). To further determine the relative contributions of TIM and TAM receptors to ZIKV infection, A549 cells that endogenously express TIM-1 and AXL, but not DC-SIGN (Fig. 5A), were infected with the virus. In keeping with the potent ZIKV infection-inducing activity of AXL, a neutralizing Ab specific for this receptor strongly inhibited viral infection of A549 cells (Fig. 5B). In contrast, the presence of a neutralizing anti-TIM-1 Ab did not have an impact on the percentage of ZIKV-infected cells at 24 hpi compared to that of cells infected with ZIKV alone. However, the combination of the anti-TIM-1 and anti-AXL Abs completely abrogated ZIKV infection (Fig. 5B). We also used the RNA silencing technique to downregulate TIM-1 and/or AXL expression in A549 cells (Fig. 5C). The results mirrored those obtained with the neutralizing Ab, in that ZIKV infection was only slightly reduced in TIM-1-silenced cells, strongly inhibited in AXL-silenced cells, and totally abrogated when both genes were silenced (Fig. 5D). Finally, to determine the importance of AXL in ZIKV infection, human skin fibroblasts that express AXL but not TIM-1 (Fig. 6A) were infected with the virus in the absence or presence of a neu-

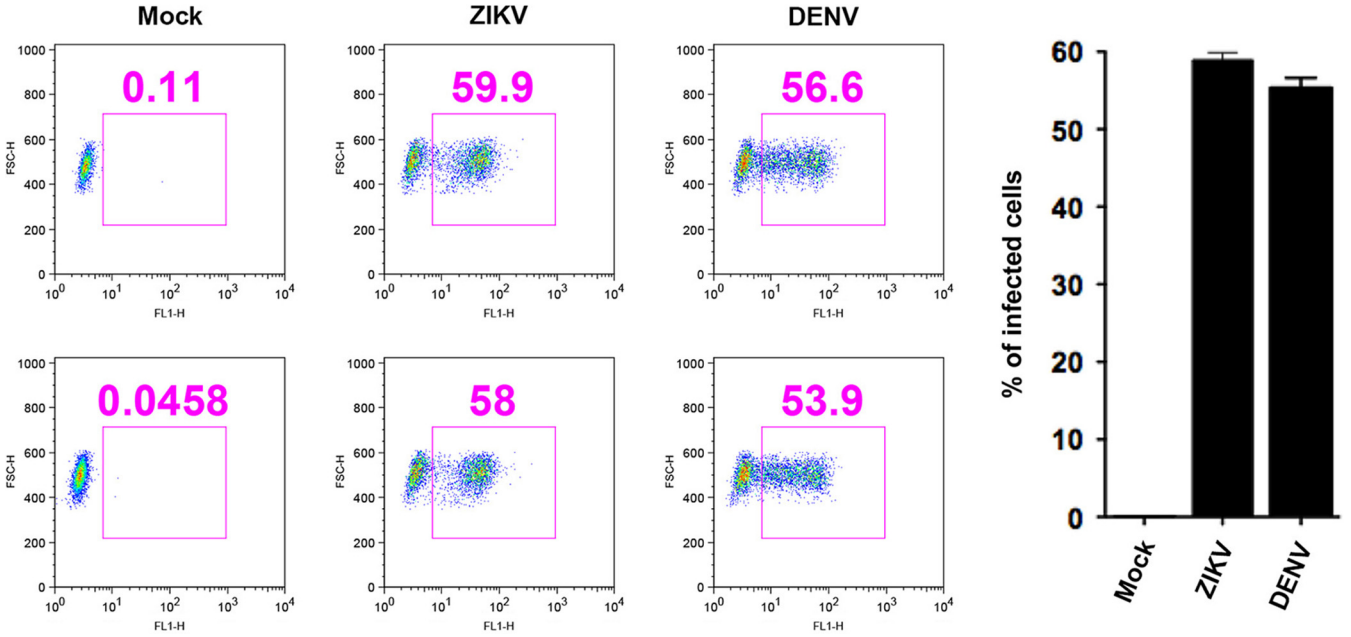

FIG 3 Dendritic cells are permissive to ZIKV and DENV. Human immature dendritic cells were infected with ZIKV or DENV (MOI = 1) for 24 hpi, and the intracellular presence of the viral envelope protein was detected using the pan-flavivirus Ab 4G2 by flow cytometry. Mean fluorescence intensities were determined, and percentages of infected cells compared to noninfected cells were calculated. Data are representative of three independent experiments.

tralizing Ab or specific siRNA. Exposure of the human skin fibroblast cell line HFF1 to ZIKV and to DENV, as a positive control, resulted in comparable numbers of infected cells that were inhibited 70% and 50%, respectively, in the presence of a neutralizing anti-AXL Ab (Fig. 6B). Strikingly, the presence of specific AXL siRNA totally inhibited AXL expression (Fig. 6C) and effectively abrogated the infection with either virus, thus demonstrating the importance of AXL in the permissiveness of human skin fibroblasts to infection and replication of ZIKV. Taken together, the data indicate an essential and cooperative role for both TIM and TAM family members in ZIKV infection of permissive cells.

ZIKV induces an innate antiviral response in primary human skin fibroblasts. In order to determine whether ZIKV induces an innate antiviral immune response in permissive cells, the antiviral gene expression profile in infected primary human fibroblasts at early time points following ZIKV infection was determined using a human qPCR array covering 84 human antiviral genes. This comparative analysis with mock-infected cells showed

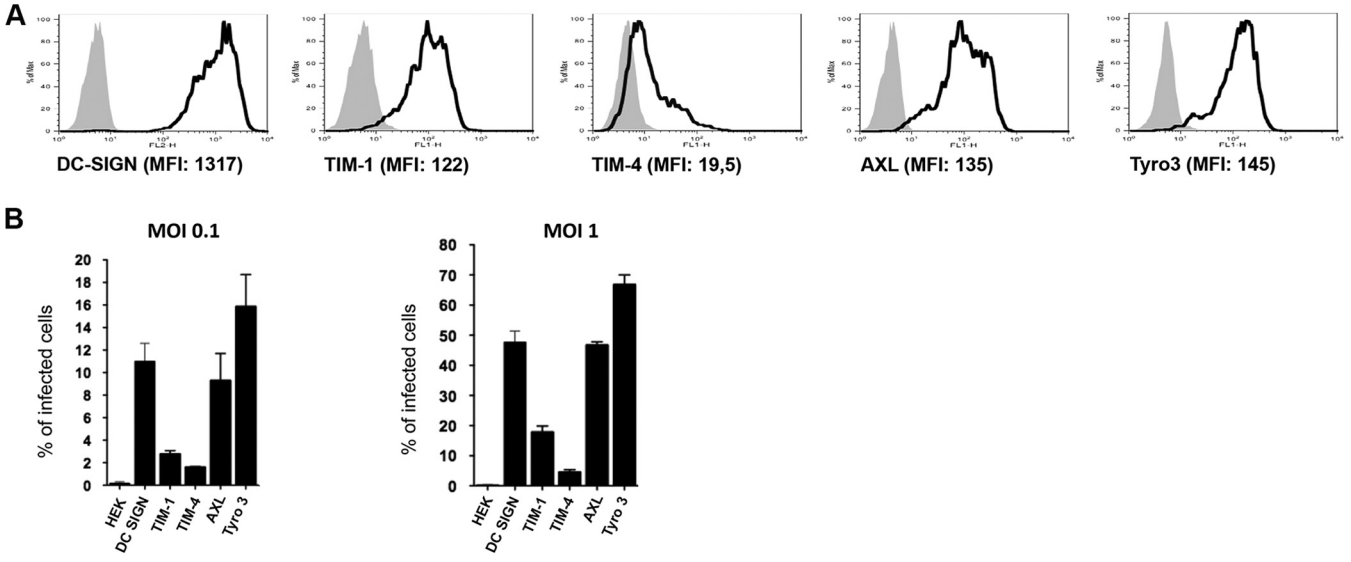

FIG 4 Entry receptors involved in ZIKV infection. (A) Expression profiles of HEK293T cells stably expressing DC-SIGN, TIM-1, TIM-4, AXL, or Tyro3 (white histograms) and of parental, nontransfected cells (gray histograms). MFI, mean fluorescence intensity. (B) HEK293T cells expressing the indicated receptors were incubated with ZIKV (MOI = 0.1 and 1), and the percentage of infected cells was determined by measuring the expression of the viral envelope protein by flow cytometry at 24 hpi. Data are representative of three independent experiments.

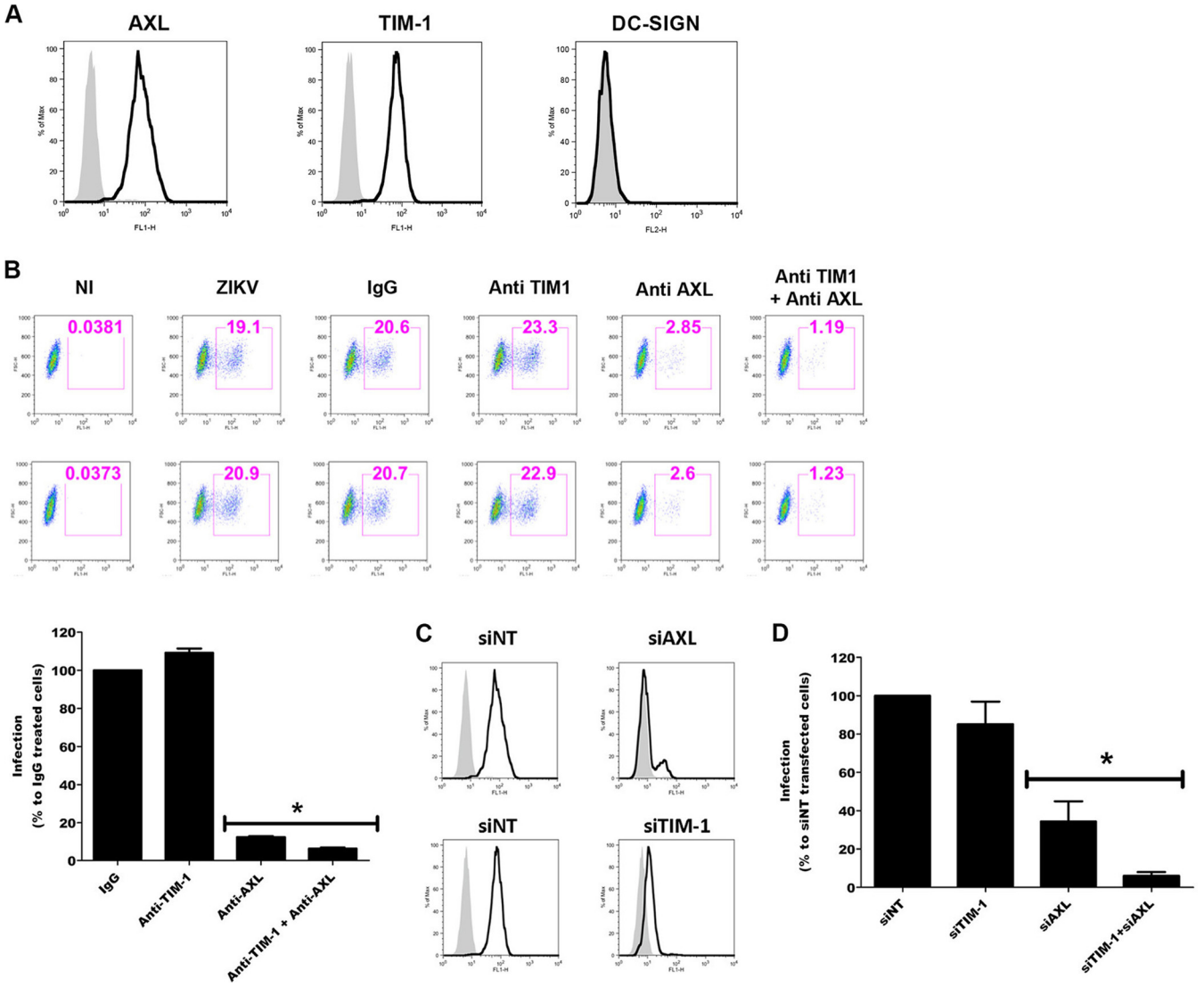

FIG 5 Involvement of AXL and TIM-1 in ZIKV infection of A549 cells. (A) Cell surface expression levels of AXL, TIM-1, and DC-SIGN on A549 cells, as determined by flow cytometry. Immunofluorescence staining of cells with a specific MAb (white histograms) is superimposed on that with an isotype control MAb (gray histograms). (B) A549 cells were incubated with ZIKV (MOI = 1) for 1 h at 4°C in the presence of neutralizing anti-TIM-1 (5 μg/ml) and/or anti-AXL (10 μg/ml) or with different concentrations of goat IgG, as a control. The percentage of infected cells was measured by flow cytometry and normalized to that in the presence of control IgG. Data shown are representative flow cytometry analysis data (upper panels) and are also presented as means ± SEM for at least three independent experiments (lower panel). (C) A549 cells were transfected with the indicated siRNA, and TIM-1 and AXL expression was assessed by flow cytometry at 24 hpi. (D) Cells were infected with ZIKV (MOI = 1). Infection was normalized to that in nontargeting (siNT) siRNA-transfected cells. To test the significance of the differences, analysis of variance (ANOVA) was performed with GraphPad Prism software. Statistically significant differences between each condition and control cells are denoted by asterisks, which indicate *P* values of <0.05. Data are representative of three independent experiments.

the specific induction of pattern recognition receptors (PRRs) able to detect the presence of pathogen-associated molecular patterns (PAMPs) in response to ZIKV infection. This is particularly illustrated by the upregulation of TLR3 mRNA expression, as well as by enhanced transcription of the DDX58 (RIG-I) and MDA5 (IFIH1) genes, which reportedly are involved in the detection of other flavivirus members (Table 1). Increased PRR expression levels and kinetics of expression during an extended time course of infection were confirmed by individual qRT-PCR analyses. As shown in Fig. 7A, RIG-I, MDA5, and TLR3 expression was upregulated in ZIKV-infected fibroblasts as soon as 6 hpi, with maximal mRNA levels detected at 48 hpi. In contrast, no activation of the TLR7 gene was observed in these cells following infection with ZIKV. The detection of viral PAMPs by TLR3 and other PRRs initiates downstream signaling pathways that account for the enhancement of transcription factors known to mobilize the antiviral machinery. The results shown in Table 1 and Fig. 7A are consistent with this general notion, as IRF7 mRNA levels were increased in ZIKV-infected cells. IRF7 is a transcription factor that binds to the interferon-stimulated response element, located on the promoters of type I IFN genes (30). This result corroborates not only the enhanced IFN-α and IFN-β gene expression detected following infection with ZIKV but also the upregulation of expression of several interferon-stimulated genes (ISGs), including

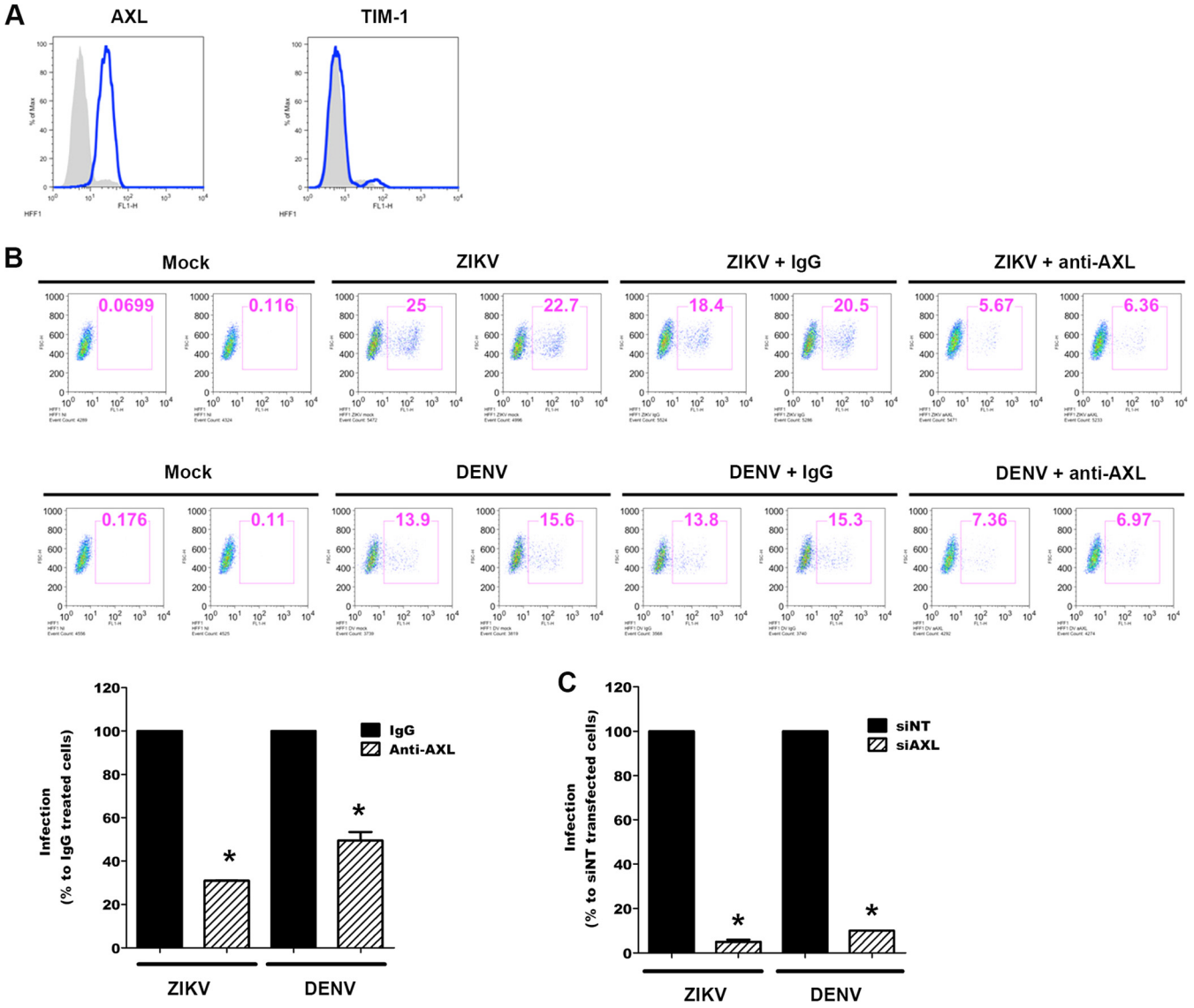

FIG 6 Expression of AXL permits ZIKV infection of skin fibroblasts. (A) Cell surface expression levels of AXL and TIM-1 on HFF1 cells were monitored by flow cytometry. Immunofluorescence staining of cells with a specific MAb (white histograms) is superimposed on those with an isotype control MAb (gray histograms). (B) HFF1 cells were incubated with ZIKV (MOI = 3) or DENV (MOI = 5) for 1 h at 4°C in the presence of neutralizing anti-AXL or normal goat IgG, as a control. The percentage of infected cells was measured by flow cytometry and normalized to that in the presence of control IgG. Data shown are representative flow cytometry analysis data (upper panels) and are presented as means ± SEM for at least three independent experiments (lower panel). (C) HFF1 cells were transfected with the indicated siRNA for 24 h, and then cells were infected with ZIKV (MOI = 3) or DENV (MOI = 5). Infection was normalized to that in nontargeting (siNT) siRNA-transfected cells. To test the significance of the differences, ANOVA was performed with GraphPad Prism software. Statistically significant differences between each condition and control cells are denoted by asterisks, which indicate *P* values of <0.05. Data are representative of three independent experiments.

OAS2, ISG15, and MX1 (Table 1 and Fig. 7B). The expression of the CXCR3 ligand CXCL10, as well as the inflammatory antiviral chemokine CCL5, was also induced by ZIKV. Finally, ZIKV infection of skin fibroblasts was also found to activate certain inflammasome components, as evidenced by a strong increase in the expression of AIM2 and interleukin-1β (IL-1β) transcripts (Fig. 7A). In order to determine the involvement of each of the upregulated PRRs in the antiviral response against ZIKV, the effects of specific siRNAs on viral replication were studied. Expression levels of MDA-5, RIG-I, TLR3, and TLR7 in HFF1 cells were decreased by 80% 24 h following the transfection of these cells with specific siRNAs and were completely inhibited after 48 h (Fig. 8A to D), thus validating the efficacy of this approach. Inhibition of TLR3 expression, unlike that of the other PRRs, resulted in a strong increase in the viral RNA copy number 48 h following viral infection of the cells (Fig. 8E). However, inhibition of TLR3 expression did not modulate type I IFN mRNA expression in the infected cells (results not shown). Taken together, these results underscore the importance of TLR3 in the induction of an antiviral response against ZIKV.

Type I and type II IFNs inhibit ZIKV replication. Because of the observed induction of type I IFNs by ZIKV-infected skin fi-

TABLE 1 Modulation of antiviral gene expression by ZIKV infection

Gene	Fold change in gene expression at indicated time postinfection[a]	
	6 h	24 h
AIM2	**5.77**	**19.67**
APOBEC3G	**3.31**	**2.64**
ATG5	−1.14	1.06
AZI2	1.24	1.96
CARD8	−1.71	−1.36
CASP1	**2.82**	**2.67**
CASP10	**3.27**	**3.31**
CASP8	1.96	1.31
CCL3	−1.71	−1.36
CCL5	1.52	**5.65**
CD40	1.90	−1.14
CD80	−1.71	−1.36
CD86	−1.71	**152.01**
CHUK	1.01	−1.16
CTSB	1.11	−1.00
CTSL1	−1.00	−1.11
CTSS	**2.48**	**2.07**
CXCL10	**−47.90**	**12.54**
CXCL11	**−6.24**	**2.05**
CXCL9	**−5.55**	−1.36
CYLD	−1.92	−1.55
DAK	**2.00**	**2.28**
DDX3X	1.27	−1.06
DDX58	**−3.16**	**4.88**
DHX58	1.76	**2.64**
FADD	−1.34	−1.08
FOS	−1.93	**2.29**
HSP90AA1	1.42	1.44
IFIH1	−1.37	**7.30**
IFNA1	**2.34**	**3.36**
IFNA2	−1.71	−1.36
IFNAR1	−1.35	−1.30
IFNB1	−1.71	**3.70**
IKBKB	1.67	1.06
IL-12A	1.53	−1.10
IL-12B	−1.73	−1.36
IL-15	−1.04	1.27
IL-18	−1.63	−1.74
IL1B	**−3.21**	**−5.29**
IL-6	1.13	**8.21**
IL-8	**−2.83**	**3.73**
IRAK1	1.40	1.61
IRF3	−1.14	−1.08
IRF5	**−2.03**	1.26
IRF7	1.25	**3.16**
ISG15	−1.10	**8.33**
JUN	**5.73**	**2.53**
MAP2K1	−1.02	−1.12
MAP2K3	−1.02	1.01
MAP3K1	**2.34**	−1.48
MAP3K7	−1.15	−1.29
MAPK1	1.26	1.01
MAPK14	1.37	−1.22
MAPK3	1.42	1.25
MAPK8	−1.21	−1.26
MAVS	−1.02	−1.53
MEFV	**−648.97**	**2.62**
MX1	1.08	**27.44**
MYD88	−1.03	1.76
NFKB1	1.22	1.63
NFKBIA	**−3.32**	1.55
NLRP3	−1.71	1.12
NOD2	−1.71	−1.36
OAS2	1.14	**16.66**
PIN1	1.62	1.09
PSTPIP1	−1.19	1.05
PYCARD	1.79	1.80
PYDC1	−1.36	−1.36
RELA	1.16	−1.05
RIPK1	1.62	1.40
SPP1	−1.88	−1.27
STAT1	1.07	1.75
SUGT1	1.28	−1.00
TBK1	−1.20	1.07
TICAM1	1.49	1.52
TLR3	**2.08**	**2.73**
TLR7	−1.71	−1.36
TLR8	−1.71	−1.36
TLR9	−1.00	**−2.25**
TNF	−1.71	**−2.13**
TRADD	1.50	1.26
TRAF3	−1.59	1.35
TRAF6	1.32	−1.13
TRIM25	1.43	1.83

[a] Values represent fold inductions of mRNA copy numbers in infected cells relative to mock-infected cells. Values in bold indicate differentially expressed genes.

broblasts, their effects on viral replication in the latter cells were investigated. Primary skin fibroblasts were pretreated for 6 h with increasing doses of recombinant human IFN-α, IFN-β, or IFN-γ and infected with ZIKV at an MOI of 1, and viral RNA copy numbers were determined by real-time PCR. At this viral titer, both type I and type II IFNs strongly and dose-dependently inhibited viral replication, with similar efficacies (Fig. 9A to C). The effects of IFNs were corroborated by a decrease in the release of viral particles, as measured by plaque assay, in the culture supernatants of the infected cells (Fig. 9D to F). These results show that ZIKV is highly sensitive to the antiviral effects of both type I and type II IFNs.

Autophagosome formation in infected skin fibroblasts increases ZIKV replication. Autophagy is a multistep process responsible for degradation and recycling of cytoplasmic components that augments the replication and dissemination of several arboviruses. We therefore analyzed whether infection of skin fibroblasts with ZIKV resulted in the formation of autophagosomes. First, an electron microscopy study was carried out to demonstrate the presence of ZIKV particles in cytoplasmic compartments as a result of exposure of cells to the virus. At 72 hpi, intravacuolar structures in ZIKV-infected fibroblasts were found to contain capsids, in combination with enveloped and electron-dense spherical viral particles that were 70 to 100 nm in diameter, which is a general feature of flavivirus particles (Fig. 10A and B). Moreover, ZIKV infection was associated with the formation of numerous double-membrane intracytoplasmic vacuoles that are characteristic of autophagosomes (Fig. 10C and D) and were not observed in mock-infected cells (results not shown). To further

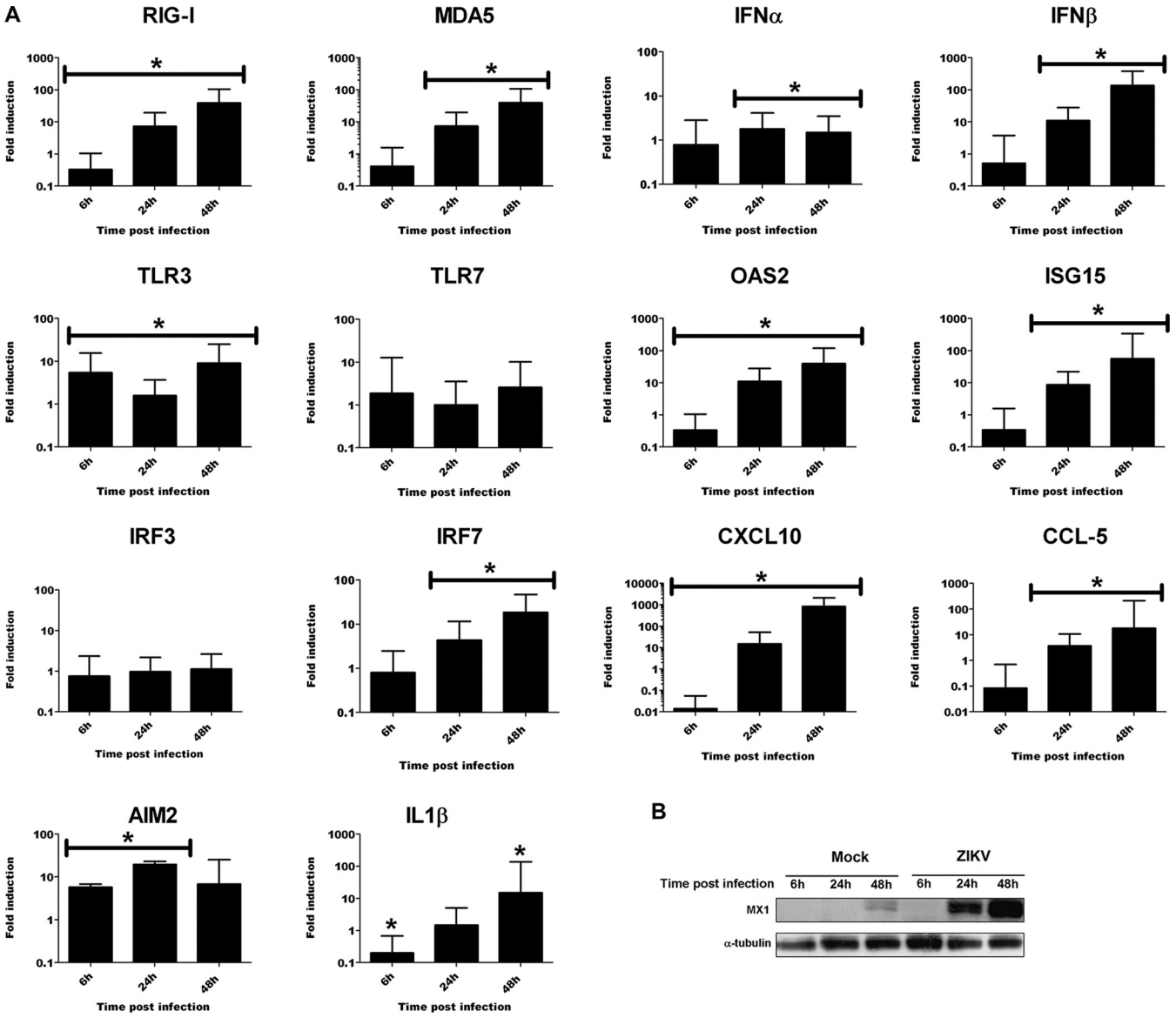

FIG 7 ZIKV induces an innate antiviral response in primary human skin fibroblasts. (A) Primary human fibroblasts were exposed to ZIKV (MOI = 1), and mRNA levels were quantified over time by real-time RT-PCR. Results are expressed as the fold induction of transcripts in ZIKV-infected cells relative to those in mock-infected cells. Data are representative of three independent experiments, each performed in duplicate (error bars represent SEM). The Wilcoxon-Mann-Whitney test was employed to analyze the differences between sets of data. *P* values of <0.05 were considered significant (*). (B) Cells were exposed to ZIKV (MOI = 1) at the indicated times, and MX1 protein levels were detected by Western blotting using a specific antibody. The immunoblot was stripped and reblotted with an anti-α-tubulin Ab as a control for protein loading. Data are representative of three independent experiments.

determine whether autophagy was induced following ZIKV infection, the skin fibroblast cell line HFF1 was infected with the virus, and the coexpression of the viral envelope protein and the cytosolic microtubule-associated light chain 3 (LC3), an autophagosome-specific marker, was determined by confocal microscopy. Torin 1, a chemical inducer of autophagy, was used as a positive control. As shown in Fig. 11A, ZIKV infection induced the formation of LC3 puncta in infected fibroblasts, while LC3 labeling was more diffuse in mock-infected cells. Interestingly, the LC3 signal in infected cells completely colocalized with that of the viral envelope protein detected by using specific antibodies. Moreover, the simultaneous addition of ZIKV and Torin 1 to primary fibroblasts enhanced viral replication, as shown by an increase in the viral RNA copy number (Fig. 11B). Conversely, addition of the 3-methyladenine (3-MA) autophagy inhibitor decreased the number of viral copies in ZIKV-infected cells, without any cytotoxic effect on the cells (results not shown), thus formally confirming the association between enhanced autophagosome formation and increased viral replication. Taken together, these results show that ZIKV is able to increase its replication via induction of autophagy in the host cell.

DISCUSSION

ZIKV is a flavivirus related to the yellow fever, dengue, West Nile, and Japanese encephalitis viruses that causes an arthropod-borne disease in humans, known as Zika fever. Originally detected in a sentinel

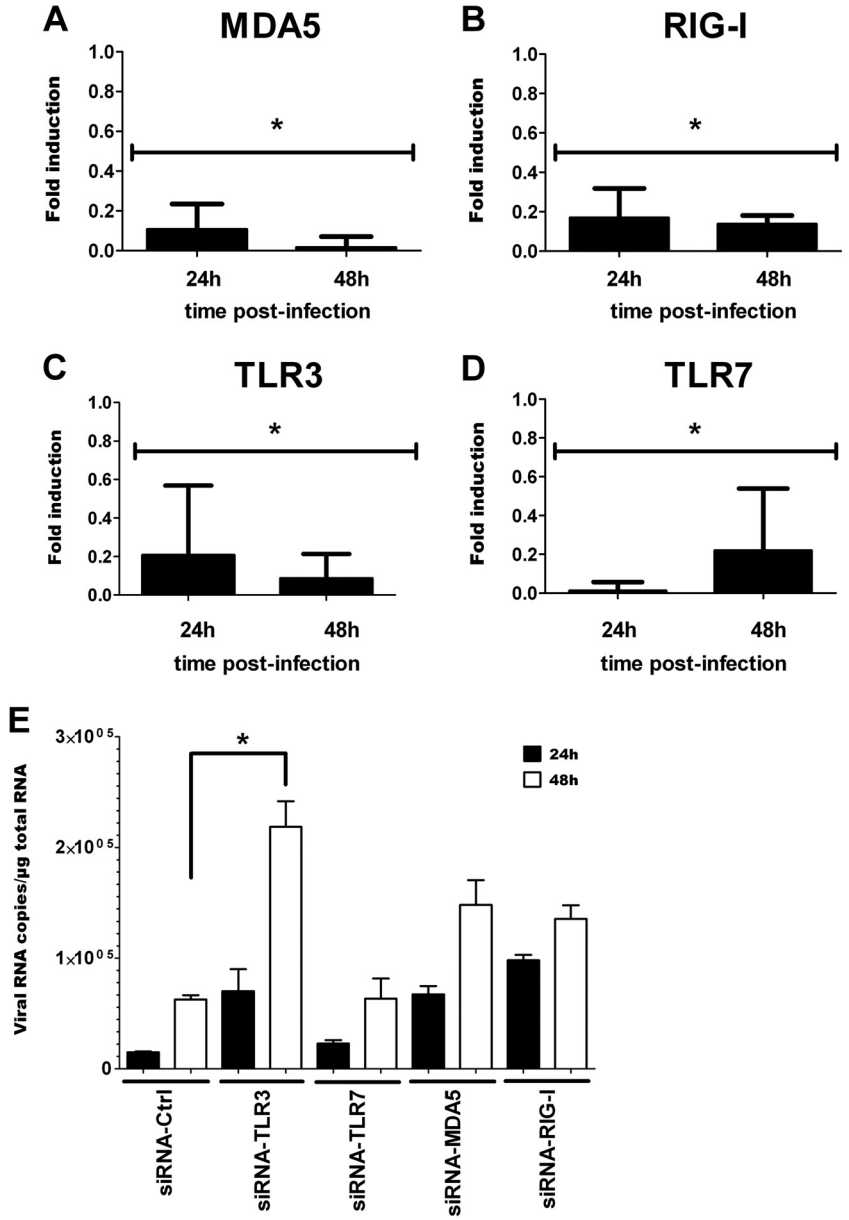

FIG 8 Effects of PRR silencing on ZIKV replication and IFN expression. (A to D) siRNAs specific for MDA5 (siRNA-MDA5), RIG-I (siRNA-RIG-I), TLR3 (siRNA-TLR3), and TLR7 (siRNA-TLR7), as well as a nonspecific siRNA (siRNA-Ctrl), were transfected into HFF1 cells 24 h before infection with ZIKV (MOI = 0.1). Reductions of mRNA levels by siRNAs were confirmed by real-time RT-PCR at 24 and 48 hpi. Results are expressed as the fold induction of expression of transcripts in specific siRNA-transfected cells relative to that in siRNA-Ctrl-transfected cells. The latter value corresponds to 1 on the ordinate of each histogram. Data are representative of two independent experiments, each performed in triplicate, and are normalized according to the 18S mRNA levels in the samples (error bars represent SEM). The Wilcoxon-Mann-Whitney test was used to analyze the differences between sets of data. *P* values of <0.05 were considered significant (*). (E) Viral copy numbers in siRNA-transfected cells were measured by real-time RT-PCR at 24 and 48 hpi. Statistically significant differences (*P* values < 0.05) between specific siRNA- and siRNA-Ctrl-transfected cells were determined by ANOVA, using GraphPad Prism software, and are denoted by an asterisk. Data are representative of two independent experiments, each performed in triplicate.

rhesus monkey in Uganda in 1947 (31), and 20 years later isolated from humans in Nigeria, the virus has since spread to other regions of the world. Importantly, following recent outbreaks in Micronesia, French Polynesia, Cook Island, and Easter Island, ZIKV has become an emerging arbovirus (18). However, other than its phylogenetic relationship to other members of the flavivirus family, no information is available on the cellular tropism of ZIKV and the nature of the cellular receptors that mediate its entry. In the present study, we identified the initial target cells of ZIKV in the skin compartment, as well as its entry receptors, and furthermore, we characterized the antiviral response elicited following infection of permissive cells with the PF-13 ZIKV strain isolated during the recent outbreak in French Polynesia (18). This strain is closely related to those isolated from patients infected during the ZIKV outbreaks in Cambodia in 2010 and Yap State in 2007 and is thus relevant to the results reported for those outbreaks as well.

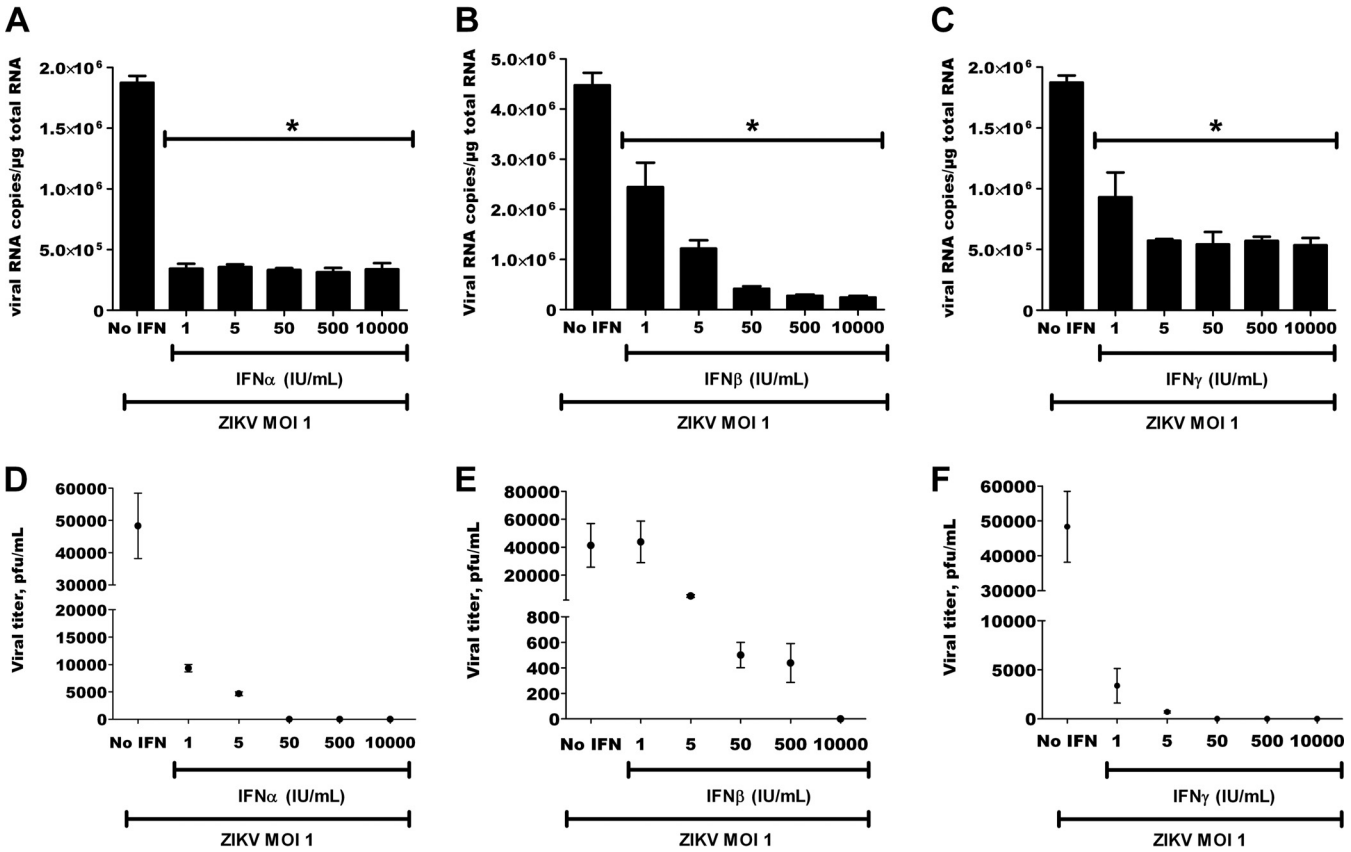

FIG 9 IFNs inhibit ZIKV infection. Primary skin fibroblasts were pretreated with different concentrations of IFN-α, IFN-β, and IFN-γ for 6 h before infection and were then exposed to ZIKV at an MOI of 1. (A to C) Inhibition of viral replication at 24 hpi was measured by real-time RT-PCR. (D to F) Release of viral particles, as quantified by plaque assay of culture supernatants. The statistical significance of the data was determined using ANOVA and GraphPad Prism software; statistically significant differences are denoted by asterisks ($P < 0.05$). Data are representative of three independent experiments, each performed in duplicate (error bars represent SEM).

ZIKV is transmitted by the *Aedes* mosquito, which deposits the virus in the epidermis and dermis of the bitten host during a blood meal. Indeed, both skin fibroblasts and epidermal keratinocytes were found to be highly permissive to infection with ZIKV. Infection of skin fibroblasts rapidly resulted in the presence of high RNA copy numbers and a gradual increase in the production of ZIKV particles over time, indicating active viral replication in the infected cells.

ZIKV infection of epidermal keratinocytes resulted in the appearance of cytoplasmic vacuolation as well as the presence of pyknotic nuclei in the stratum granulosum, which is indicative of cells undergoing apoptosis. This bears similarity to observations made with DENV, which induces the appearance of apoptotic cells in the epidermis of infected human skin explants (27). It can be speculated that the induction of apoptotic cell death is a mechanism by which ZIKV, like DENV, is able to divert antiviral immune responses by increasing their dissemination from dying cells. These results also corroborate previous reports in the literature showing the importance of keratinocytes in infections with other flaviviruses, such as WNV (32) and DENV (25). In addition to dermal fibroblasts and epidermal keratinocytes, we report that dendritic cells are permissive to infection with ZIKV. This comes as no surprise given the involvement of skin antigen-presenting cells in the replication of other flavivirus members, in particular DENV, which efficiently infects Langerhans cells (33). However, the selective susceptibility of permissive cells in the dermis and epidermis, including Langerhans cells, dermal dendritic cells, macrophages, fibroblasts, and keratinocytes, to infection with ZIKV needs to be determined.

The first step of flavivirus entry into a host cell is mediated by the viral envelope protein, which interacts with several cell surface receptors and attachment factors, whose differential expression determines the cellular tropism of the virus. At present, more than a dozen putative entry receptors and factors, in particular for DENV, have been described. Several of them, such as heat shock proteins, laminin receptor, integrin αvβ3, prohibitin, claudin-1, scavenger receptor class B, and natural killer cell receptor NKp44, can interact with viral particles in mammalian and/or mosquito cells, but their exact role in the flavivirus entry program, as well as their physiologic relevance, is not well understood (reviewed in reference 29). Heparan sulfate, a sulfated polysaccharide associated with proteins from the extracellular matrix, has been described as a nonspecific attachment factor of flaviviruses, as it concentrates viral particles on the cell surface and facilitates their interaction with primary receptors (34–38). Among them, C-type lectin receptors, such as the dendritic cell-specific intracellular adhesion molecule 3-grabbing nonintegrin (DC-SIGN; also called CD209), the mannose receptor, and the C-type lectin domain

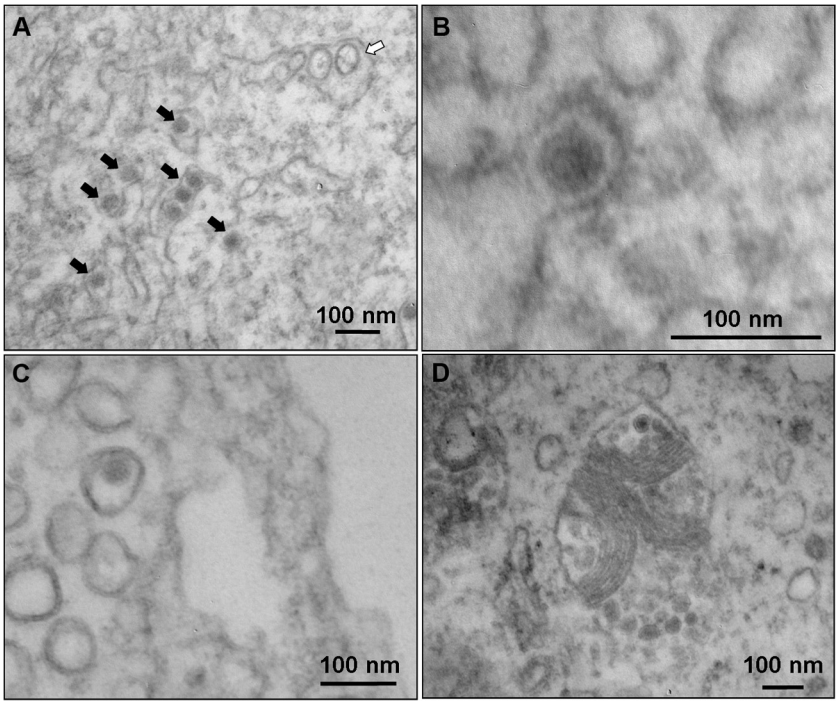

FIG 10 Electron microscopic imaging of ZIKV-infected primary fibroblasts. (A) Membrane vesicles with sizes between 70 and 100 nm, observed in intimate association with the endoplasmic reticulum, are indicated by a white arrow. Black arrows indicate the presence of spherical capsids detected in intracellular vacuoles or docked to intracellular membranes. (B) Enlargement of a ZIKV particle. The intracellular electron-dense spherical capsid is 40 nm in diameter. (C) Assembled capsids are transported to the cell surface in intracellular vacuoles. (D) Autophagosomes are frequently detected in infected fibroblasts, and assembled capsids are observed inside this compartment. Data are representative of two independent experiments.

family 5 member A (CLEC5A; also called MDL-1), play an important role in flavivirus binding and infection of myeloid cells (39–41). Recently, TIM and TAM proteins, two distinct families of transmembrane receptors that participate in the phosphatidylserine-dependent phagocytic engulfment and removal of apoptotic cells, have also been shown to act as DENV entry factors, promoting viral infection by attaching to and possibly internalizing viral particles in human cell cultures and primary cells targeted by flaviviruses (26, 29).

We show here that ZIKV entry is mediated by DC-SIGN, AXL, Tyro3, and, to a lesser extent, TIM-1. Although TIM-1 by itself contributed little to ZIKV infection, its expression nevertheless had an additive effect on the efficacy of AXL-mediated viral entry. This raises the interesting possibility of a cooperation between both receptors, with TIM-1 acting as an attachment factor that binds viral particles and transfers them to AXL, which could in turn participate in viral internalization. In that sense, TIM-1 might not be indispensable for ZIKV endocytosis and infection but rather would concentrate virions on the cell surface to facilitate their interaction with AXL, as well as the subsequent infection, which might explain the additive inhibitory effect observed when both receptors are blocked by use of neutralizing antibodies. However, additional experiments are required to assess the exact role in ZIKV infection played by TIM and TAM receptors.

As has been reported for DENV, there seems to be a large number of receptors and/or attachment factors that are able to mediate entry of ZIKV into permissive cells. Note, however, that the permissiveness of skin cells to ZIKV is also determined by the profile of receptor expression by these target cells. In this respect, unlike immature dendritic cells, which are also a primary target cell type for ZIKV infection, neither cutaneous fibroblasts nor epidermal keratinocytes express DC-SIGN. In contrast, the latter cells, as well as macrophages, vascular endothelium cells, and astrocytes (reviewed in reference 42), express AXL, which was shown in the present study to have major importance for ZIKV entry. The availability of different entry receptors is likely to provide an evolutionary advantage for the virus, and as a result, the virus is able to infect a wide range of target cells and invade the human host. Nevertheless, the contribution of each of these receptors and/or attachment factors to ZIKV infection and pathogenesis is currently unknown and remains to be established. It is also important to consider that other, as yet unidentified cell surface molecules may exist that might account for the tropism of ZIKV.

The outcome of viral infection is determined by a competition between viral replication and the host immune response. The latter is programmed to rapidly control viral replication and to limit virus spread by recognizing nonself nucleic acids as PAMPs, triggering an antiviral response. Indeed, infection of fibroblasts *in vitro* with ZIKV strongly induced the expression of several antiviral gene clusters, in particular those for PRRs, such as RIG-I, MDA-5, and TLR3, that are able to detect the presence of PAMPs. These results corroborate previous reports in the literature showing that these gene products play a sensory role in the detection of other flaviviruses, such as DENV and WNV (25, 43). The induction of TLR3 expression is rapid and already detectable at 6 hpi, whereas that of RIG-I and MDA-5 is delayed. It can therefore be hypothesized that these molecules trigger a coordinated induction of the antiviral immune reaction against ZIKV, with TLR3 prim-

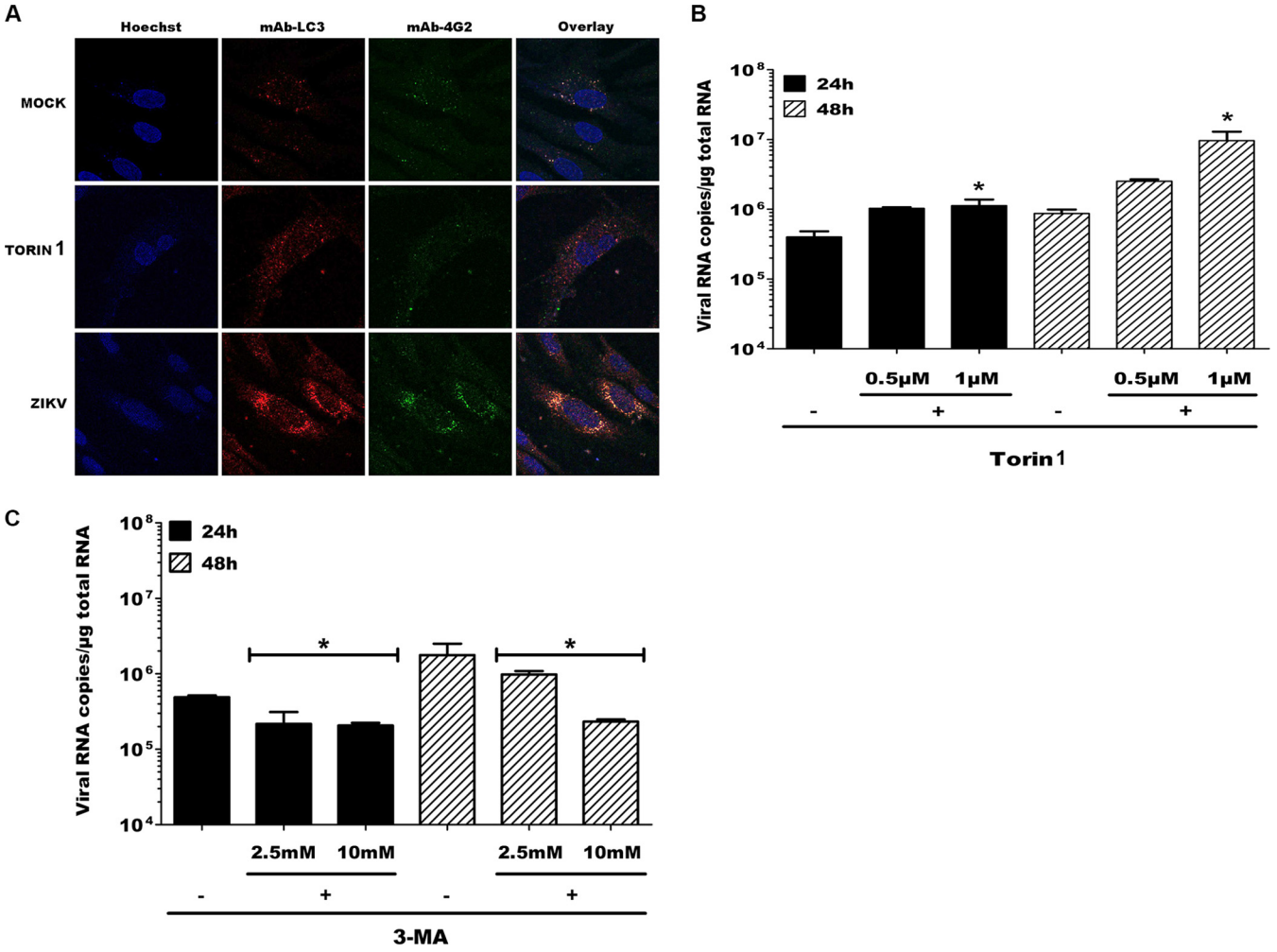

FIG 11 ZIKV induces autophagy in infected skin fibroblasts. (A) Visualization of autophagosome formation by LC3 aggregation in mock- or ZIKV-infected cells and cells treated with Torin 1. Cells were fixed at 24 hpi, and the colocalization of autophagosomes and ZIKV was determined by immunofluorescence, using MAbs specific for LC3 or the viral envelope protein (4G2). Data are representative of three independent experiments. (B and C) Primary human skin fibroblasts were exposed to ZIKV (MOI = 2) in the absence (cells were treated with the vehicle [0.05% dimethyl sulfoxide]) or presence of Torin 1 (B) or 3-MA (C), at the indicated concentrations, and viral replication was quantified by real-time RT-PCR at 24 and 48 hpi. Data are representative of three independent experiments. To test the significance of the differences, ANOVA was performed with GraphPad Prism software. Statistically significant differences between each condition and control cells are denoted by asterisks ($P < 0.05$).

ing an early response that is amplified by RIG-I and MDA-5 at a later stage. This sequence of events has also been suggested previously with respect to the immune response of fibroblasts following infection with DENV (44). However, in that study, the involvement of only TLR3 and RIG-I was considered, because, in contrast to ZIKV infection, DENV infection did not enhance the expression of MDA5 in skin fibroblasts.

Both TLR3 and TLR7 are implicated in the induction of an immune response against flaviviruses, and triggering of these PRRs has been shown to initiate signaling pathways leading to the production of type I IFNs, as well as other inflammatory cytokines and chemokines, by hepatocytes and macrophages (reviewed in reference 45). Indeed, ZIKV infection strongly enhanced TLR3 expression, in association with the production of IFN-α and IFN-β in infected cells. However, whereas inhibition of TLR3 expression by siRNA indeed resulted in a strong enhancement of viral replication, no effect on type I IFN mRNA expression was detected. Although TLR3 seems to play an important role in the antiviral response to ZIKV, the mechanism by which this receptor contributes to the control of viral replication remains to be determined. In contrast, no modulation of TLR7 expression was observed, which is reminiscent of results obtained with DENV-infected skin fibroblasts (44). The absence of TLR7 induction was also reported in a separate study, in which expression of PRRs in virally infected fibroblasts of different origins was analyzed (46). Taken together, these findings confirm the notion that the involvement of various TLR members seems to be dependent on the virus and cell type.

The detection of ZIKV-expressed PAMPs also resulted in an increase in transcriptional levels of IRF7, a transcription factor that binds to the interferon-stimulated response element, located on the promoters of type I IFN genes (30). This result corroborates the enhanced IFN-α and IFN-β gene expression detected following infection with ZIKV, as well as the upregulation of expression

of several interferon-stimulated genes, including OAS2, ISG15, and MX1. The expression of the two CXCR3 ligands, CXCL10 and CXCL11, was also induced by ZIKV. The latter chemokines not only play a role in innate and adaptive immunity by attracting T cells and other leukocytes to sites of inflammation but also display direct, receptor-independent, defensin-like antimicrobial activity when present at elevated concentrations in dermal fibroblasts (47). In addition, infection of skin fibroblasts by ZIKV resulted in upregulation of CCL5, another inflammatory chemokine that is known for its antiviral activity.

Whereas TLR3 transcription was significantly enhanced, IRF3 gene expression, in contrast, remained unchanged during the course of ZIKV infection of fibroblasts. A similar observation was made in DENV-infected epidermal keratinocytes, in which no enhanced IRF3 expression could be detected. This is somewhat surprising because IRF3 is known to play an important role in the induction of IFN-β production in cells exposed to PAMPs from various viruses (48). Moreover, double-stranded RNA (dsRNA)-mediated triggering of RIG-I and MDA5, both molecules whose expression is upregulated following infection with ZIKV and other flaviviruses, seems to be crucial for IRF3 activation (25). It has been reported that IFN-β production, which is essential for the early antiviral immune response, was observed in both wild-type and IRF3$^{-/-}$ mice following WNV infection (48). These results corroborate the present and previously published data (25) indicating that the production of type I IFNs in response to DENV or ZIKV infection is apparently independent of the IRF3 pathway in both flavivirus-infected epidermal keratinocytes and skin fibroblasts. Note that the replication of ZIKV was significantly inhibited by both type I and type II IFNs, in keeping with the general antiviral activity of these cytokines with critical functions in host defense mechanisms.

Electron microscopy analysis of ZIKV-infected primary skin fibroblasts showed the presence of membrane vesicles of 70 to 100 nm that were located in intimate association with the endoplasmic reticulum, indicating that ZIKV replication occurs in close association with host cell membranes. These results are in line with an earlier report in the literature underscoring the importance of fibroblasts as a primary cell type of replication for flaviviruses, such as DENV, that, through the release of viral particles, may contribute to subsequent viral dissemination (44). ZIKV infection also induced an autophagy program, as demonstrated by the presence of characteristic autophagosome-like vesicles in the infected fibroblasts. Autophagy is a process characterized by the presence of double-membrane vesicles, known as autophagosomes, that recruit cytoplasmic material and subsequently fuse with lysosomes for protein degradation. Autophagy not only participates in the degradation of proteins and damaged organelles in the cytoplasm to maintain homeostasis (49) but also is involved in host immunity against pathogen infection. This is particularly illustrated by vesicular stomatitis virus (50)-, Sendai virus (51)-, and herpes simplex virus 1 (52)-infected cells, in which autophagy-mediated degradation of viral proteins limits viral replication and promotes cell survival. In contrast, the autophagy process can be subverted by viruses. This is true for several arboviruses, including DENV (53, 54), Chikungunya virus (55), and Japanese encephalitis virus (56), that use components of the autophagy pathway to promote their replication and dissemination by clearing cells through multiple mechanisms. In this regard, autophagy may thus have both pro- and antiviral effects.

Autophagy in ZIKV-infected fibroblasts was furthermore confirmed by the demonstration of colocalization of the viral envelope protein and the cytosolic microtubule-associated molecule LC3. The results also showed that stimulation of autophagosome formation by Torin 1 further enhanced the replication of ZIKV in permissive cells, whereas the presence of 3-MA, an inhibitor of autophagosome formation, strongly reduced viral copy numbers in the infected fibroblasts, indicating that autophagy promotes the replication of ZIKV in permissive cells. In this respect, ZIKV behaves like most other flavivirus members, with the exception of WNV (57), by its capacity to interact with the conventional autophagy pathway in mammalian cells. The precise mechanism by which ZIKV induces autophagy still needs to be determined. Nevertheless, similar to the findings for DENV (58), the results from our study demonstrating the colocalization of ZIKV with LC3 strongly suggest that autophagocytic vacuoles are the site of viral replication. It can furthermore be speculated that autophagy may promote replication of ZIKV infection through restriction of the antiviral innate immune response (59), by enhancement of translation of the viral genome that has entered the mammalian cells (60), or by providing additional energy and relevant membrane structures for viral replication (61). However, the exact molecular mechanism(s) by which ZIKV highjacks components of the autophagosome pathways remains to be determined.

At present, ZIKV has received far less attention in the literature than the other mosquito-borne flavivirus members. Nevertheless, it is considered to be an emerging virus because of its global spreading during the last decades and its pathogenic potential, which is reminiscent of that of DENV. Importantly, ZIKV was recently isolated in Gabon, from the Asian tiger mosquito *A. albopictus* (62), a rapidly expanding *Aedes* species that lives in close contact with human urban populations (63, 64) and that typically feeds not only at dusk and dawn but also in the daytime. This underscores its menacing character, as this vector is known for its capacity to colonize new environments, either by progressive extension from already occupied zones or by jumping to new areas, in particular to those in heavily populated urban areas. In this respect, a better understanding of the role of mosquito saliva in ZIKV infection is an important point that must be addressed in the future as well.

Taken together, the results presented in this study pertaining to the identification of the cellular tropism and molecular mechanisms of infection and replication of ZIKV, as well as the signaling pathways involved in the antiviral immune response to this virus, permit us to gain better insight into its mode of action and to devise strategies aiming to interfere with the pathology caused by this emerging flavivirus.

ACKNOWLEDGMENTS

We thank François Renaud for critical discussions, Chantal Cazevieille for expert help with electron microscopy, and Eric Bernard for technical assistance.

This work was supported by grants from the Agence Nationale de la Recherche (grants ANR-12-BSV3-0004-01 and ANR-14-CE14-0029). Sineewanlaya Wichit was supported by a fellowship from the Infectiopôle Sud foundation.

The funders had no role in study design, data collection and analysis, decision to publish, or preparation of the manuscript.

REFERENCES

1. **Kuno G, Chang GJ, Tsuchiya KR, Karabatsos N, Cropp CB.** 1998. Phylogeny of the genus Flavivirus. J Virol **72:**73–83.
2. **Moore DL, Causey OR, Carey DE, Reddy S, Cooke AR, Akinkugbe FM, David-West TS, Kemp GE.** 1975. Arthropod-borne viral infections of man in Nigeria, 1964–1970. Ann Trop Med Parasitol **69:**49–64.
3. **Simpson DI.** 1964. Zika virus infection in man. Trans R Soc Trop Med Hyg **58:**335–338. http://dx.doi.org/10.1016/0035-9203(64)90200-7.
4. **Smithburn KC.** 1954. Neutralizing antibodies against arthropod-borne viruses in the sera of long-time residents of Malaya and Borneo. Am J Hyg **59:**157–163.
5. **Fagbami AH.** 1979. Zika virus infections in Nigeria: virological and sero-epidemiological investigations in Oyo State. J Hyg **83:**213–219. http://dx.doi.org/10.1017/S0022172400025997.
6. **Hammon WM, Schrack WD, Sather GE.** 1958. Serological survey for a arthropod-borne virus infections in the Philippines. Am J Trop Med Hyg **7:**323–328.
7. **Pond WL.** 1963. Arthropod-borne virus antibodies in sera from residents of South-East Asia. Trans R Soc Trop Med Hyg **57:**364–371. http://dx.doi.org/10.1016/0035-9203(63)90100-7.
8. **Olson JG, Ksiazek TG, Suhandiman, Triwibowo.** 1981. Zika virus, a cause of fever in Central Java, Indonesia. Trans R Soc Trop Med Hyg **75:**389–393. http://dx.doi.org/10.1016/0035-9203(81)90100-0.
9. **Darwish MA, Hoogstraal H, Roberts TJ, Ghazi R, Amer T.** 1983. A sero-epidemiological survey for Bunyaviridae and certain other arboviruses in Pakistan. Trans R Soc Trop Med Hyg **77:**446–450. http://dx.doi.org/10.1016/0035-9203(83)90108-6.
10. **Marchette NJ, Garcia R, Rudnick A.** 1969. Isolation of Zika virus from Aedes aegypti mosquitoes in Malaysia. Am J Trop Med Hyg **18:**411–415.
11. **Li MI, Wong PS, Ng LC, Tan CH.** 2012. Oral susceptibility of Singapore Aedes (Stegomyia) aegypti (Linnaeus) to Zika virus. PLoS Negl Trop Dis **6:**e1792. http://dx.doi.org/10.1371/journal.pntd.0001792.
12. **Boorman JP, Porterfield JS.** 1956. A simple technique for infection of mosquitoes with viruses; transmission of Zika virus. Trans R Soc Trop Med Hyg **50:**238–242. http://dx.doi.org/10.1016/0035-9203(56)90029-3.
13. **Monlun E, Zeller H, Le Guenno B, Traoré-Lamizana M, Hervy JP, Adam F, Ferrara L, Fontenille D, Sylla R, Mondo M.** 1993. Surveillance of the circulation of arbovirus of medical interest in the region of eastern Senegal. Bull Soc Pathol Exot **86:**21–28.
14. **Weinbren MP, Williams MC.** 1958. Zika virus: further isolations in the Zika area, and some studies on the strains isolated. Trans R Soc Trop Med Hyg **52:**263–268. http://dx.doi.org/10.1016/0035-9203(58)90085-3.
15. **Haddow AJ, Williams MC, Woodall JP, Simpson DI, Goma LK.** 1964. Twelve isolations of Zika virus from Aedes (Stegomyia) africanus (Theobald) taken in and above a Uganda forest. Bull World Health Organ **31:**57–69.
16. **Haddow AD, Schuh AJ, Yasuda CY, Kasper MR, Heang V, Huy R, Guzman H, Tesh RB, Weaver SC.** 2012. Genetic characterization of Zika virus strains: geographic expansion of the Asian lineage. PLoS Negl Trop Dis **6:**e1477. http://dx.doi.org/10.1371/journal.pntd.0001477.
17. **Duffy MR, Chen TH, Hancock WT, Powers AM, Kool JL, Lanciotti RS, Pretrick M, Marfel M, Holzbauer S, Dubray C, Guillaumot L, Griggs A, Bel M, Lambert AJ, Laven J, Kosoy O, Panella A, Biggerstaff BJ, Fischer M, Hayes EB.** 2009. Zika virus outbreak on Yap Island, Federated States of Micronesia. N Engl J Med **360:**2536–2543. http://dx.doi.org/10.1056/NEJMoa0805715.
18. **Musso D, Nilles EJ, Cao-Lormeau VM.** 2014. Rapid spread of emerging Zika virus in the Pacific area. Clin Microbiol Infect **20:**O595–O596. http://dx.doi.org/10.1111/1469-0691.12707.
19. **Kwong JC, Druce JD, Leder K.** 2013. Zika virus infection acquired during brief travel to Indonesia. Am J Trop Med Hyg **89:**516–517. http://dx.doi.org/10.4269/ajtmh.13-0029.
20. **Tappe D, Rissland J, Gabriel M, Emmerich P, Gunther S, Held G, Smola S, Schmidt-Chanasit J.** 2014. First case of laboratory-confirmed Zika virus infection imported into Europe, November 2013. Euro Surveill **19:**20685.
21. **Pyke AT, Daly MT, Cameron JN, Moore PR, Taylor CT, Hewitson GR, Humphreys JL, Gair R.** 2014. Imported Zika virus infection from the Cook Islands into Australia, 2014. PLoS Curr **6:**ecurrents.outbreaks.4635a54dbffba2156fb2fd76dc49f65e. http://dx.doi.org/10.1371/currents.outbreaks.4635a54dbffba2156fb2fd76dc49f65e.
22. **Fonseca K, Meatherall B, Zarra D, Drebot M, MacDonald J, Pabbaraju K, Wong S, Webster P, Lindsay R, Tellier R.** 2014. First case of Zika virus infection in a returning Canadian traveler. Am J Trop Med Hyg **91:**1035–1038. http://dx.doi.org/10.4269/ajtmh.14-0151.
23. **Oehler E, Watrin L, Larre P, Leparc-Goffart I, Lastere S, Valour F, Baudouin L, Mallet H, Musso D, Ghawche F.** 2014. Zika virus infection complicated by Guillain-Barre syndrome—case report, French Polynesia, December 2013. Euro Surveill **19:**20720.
24. **Briant L, Desprès P, Choumet V, Missé D.** 2014. Role of skin immune cells on the host susceptibility to mosquito-borne viruses. Virology **464–465:**26–32. http://dx.doi.org/10.1016/j.virol.2014.06.023.
25. **Surasombatpattana P, Hamel R, Patramool S, Luplertlop N, Thomas F, Despres P, Briant L, Yssel H, Misse D.** 2011. Dengue virus replication in infected human keratinocytes leads to activation of antiviral innate immune responses. Infect Genet Evol **11:**1664–1673. http://dx.doi.org/10.1016/j.meegid.2011.06.009.
26. **Meertens L, Carnec X, Lecoin MP, Ramdasi R, Guivel-Benhassine F, Lew E, Lemke G, Schwartz O, Amara A.** 2012. The TIM and TAM families of phosphatidylserine receptors mediate dengue virus entry. Cell Host Microbe **12:**544–557. http://dx.doi.org/10.1016/j.chom.2012.08.009.
27. **Limon-Flores AY, Perez-Tapia M, Estrada-Garcia I, Vaughan G, Escobar-Gutierrez A, Calderon-Amador J, Herrera-Rodriguez SE, Brizuela-Garcia A, Heras-Chavarria M, Flores-Langarica A, Cedillo-Barron L, Flores-Romo L.** 2005. Dengue virus inoculation to human skin explants: an effective approach to assess in situ the early infection and the effects on cutaneous dendritic cells. Int J Exp Pathol **86:**323–334. http://dx.doi.org/10.1111/j.0959-9673.2005.00445.x.
28. **Lanciotti RS, Kosoy OL, Laven JJ, Velez JO, Lambert AJ, Johnson AJ, Stanfield SM, Duffy MR.** 2008. Genetic and serologic properties of Zika virus associated with an epidemic, Yap State, Micronesia, 2007. Emerg Infect Dis **14:**1232–1239. http://dx.doi.org/10.3201/eid1408.080287.
29. **Perera-Lecoin M, Meertens L, Carnec X, Amara A.** 2014. Flavivirus entry receptors: an update. Viruses **6:**69–88. http://dx.doi.org/10.3390/v6010069.
30. **Honda K, Yanai H, Negishi H, Asagiri M, Sato M, Mizutani T, Shimada N, Ohba Y, Takaoka A, Yoshida N, Taniguchi T.** 2005. IRF-7 is the master regulator of type-I interferon-dependent immune responses. Nature **434:**772–777. http://dx.doi.org/10.1038/nature03464.
31. **Dick GW, Kitchen SF, Haddow AJ.** 1952. Zika virus. I. Isolations and serological specificity. Trans R Soc Trop Med Hyg **46:**509–520. http://dx.doi.org/10.1016/0035-9203(52)90042-4.
32. **Lim PY, Behr MJ, Chadwick CM, Shi PY, Bernard KA.** 2011. Keratinocytes are cell targets of West Nile virus in vivo. J Virol **85:**5197–5201. http://dx.doi.org/10.1128/JVI.02692-10.
33. **Cerny D, Haniffa M, Shin A, Bigliardi P, Tan BK, Lee B, Poidinger M, Tan EY, Ginhoux F, Fink K.** 2014. Selective susceptibility of human skin antigen presenting cells to productive dengue virus infection. PLoS Pathog **10:**e1004548. http://dx.doi.org/10.1371/journal.ppat.1004548.
34. **Chen Y, Maguire T, Hileman RE, Fromm JR, Esko JD, Linhardt RJ, Marks RM.** 1997. Dengue virus infectivity depends on envelope protein binding to target cell heparan sulfate. Nat Med **3:**866–871. http://dx.doi.org/10.1038/nm0897-866.
35. **Germi R, Crance JM, Garin D, Guimet J, Lortat-Jacob H, Ruigrok RW, Zarski JP, Drouet E.** 2002. Heparan sulfate-mediated binding of infectious dengue virus type 2 and yellow fever virus. Virology **292:**162–168. http://dx.doi.org/10.1006/viro.2001.1232.
36. **Hilgard P, Stockert R.** 2000. Heparan sulfate proteoglycans initiate dengue virus infection of hepatocytes. Hepatology **32:**1069–1077. http://dx.doi.org/10.1053/jhep.2000.18713.
37. **Kroschewski H, Allison SL, Heinz FX, Mandl CW.** 2003. Role of heparan sulfate for attachment and entry of tick-borne encephalitis virus. Virology **308:**92–100. http://dx.doi.org/10.1016/S0042-6822(02)00097-1.
38. **Lee E, Pavy M, Young N, Freeman C, Lobigs M.** 2006. Antiviral effect of the heparan sulfate mimetic, PI-88, against dengue and encephalitic flaviviruses. Antiviral Res **69:**31–38. http://dx.doi.org/10.1016/j.antiviral.2005.08.006.
39. **Navarro-Sanchez E, Altmeyer R, Amara A, Schwartz O, Fieschi F, Virelizier JL, Arenzana-Seisdedos F, Despres P.** 2003. Dendritic-cell-specific ICAM3-grabbing non-integrin is essential for the productive infection of human dendritic cells by mosquito-cell-derived dengue viruses. EMBO Rep **4:**723–728. http://dx.doi.org/10.1038/sj.embor.embor866.
40. **Tassaneetrithep B, Burgess TH, Granelli-Piperno A, Trumpfheller C, Finke J, Sun W, Eller MA, Pattanapanyasat K, Sarasombath S, Birx DL, Steinman RM, Schlesinger S, Marovich MA.** 2003. DC-SIGN (CD209)

mediates dengue virus infection of human dendritic cells. J Exp Med **197:** 823–829. http://dx.doi.org/10.1084/jem.20021840.
41. **Chen ST, Lin YL, Huang MT, Wu MF, Cheng SC, Lei HY, Lee CK, Chiou TW, Wong CH, Hsieh SL.** 2008. CLEC5A is critical for dengue-virus-induced lethal disease. Nature **453:**672–676. http://dx.doi.org/10.1038/nature07013.
42. **Lemke G, Rothlin CV.** 2008. Immunobiology of the TAM receptors. Nat Rev Immunol **8:**327–336. http://dx.doi.org/10.1038/nri2303.
43. **Fredericksen BL, Keller BC, Fornek J, Katze MG, Gale M.** 2008. Establishment and maintenance of the innate antiviral response to West Nile virus involves both RIG-I and MDA5 signaling through IPS-1. J Virol **82:**609–616. http://dx.doi.org/10.1128/JVI.01305-07.
44. **Bustos-Arriaga J, Garcia-Machorro J, Leon-Juarez M, Garcia-Cordero J, Santos-Argumedo L, Flores-Romo L, Mendez-Cruz AR, Juarez-Delgado FJ, Cedillo-Barron L.** 2011. Activation of the innate immune response against DENV in normal non-transformed human fibroblasts. PLoS Negl Trop Dis **5:**e1420. http://dx.doi.org/10.1371/journal.pntd.0001420.
45. **Nazmi A, Dutta K, Hazra B, Basu A.** 2014. Role of pattern recognition receptors in flavivirus infections. Virus Res **185:**32–40. http://dx.doi.org/10.1016/j.virusres.2014.03.013.
46. **Paladino P, Cummings DT, Noyce RS, Mossman KL.** 2006. The IFN-independent response to virus particle entry provides a first line of antiviral defense that is independent of TLRs and retinoic acid-inducible gene I. J Immunol **177:**8008–8016. http://dx.doi.org/10.4049/jimmunol.177.11.8008.
47. **Proost P, Vynckier AK, Mahieu F, Put W, Grillet B, Struyf S, Wuyts A, Opdenakker G, Van Damme J.** 2003. Microbial Toll-like receptor ligands differentially regulate CXCL10/IP-10 expression in fibroblasts and mononuclear leukocytes in synergy with IFN-gamma and provide a mechanism for enhanced synovial chemokine levels in septic arthritis. Eur J Immunol **33:**3146–3153. http://dx.doi.org/10.1002/eji.200324136.
48. **Bourne N, Scholle F, Silva MC, Rossi SL, Dewsbury N, Judy B, De Aguiar JB, Leon MA, Estes DM, Fayzulin R, Mason PW.** 2007. Early production of type I interferon during West Nile virus infection: role for lymphoid tissues in IRF3-independent interferon production. J Virol **81:** 9100–9108. http://dx.doi.org/10.1128/JVI.00316-07.
49. **Xie Z, Klionsky DJ.** 2007. Autophagosome formation: core machinery and adaptations. Nat Cell Biol **9:**1102–1109. http://dx.doi.org/10.1038/ncb1007-1102.
50. **Shelly S, Lukinova N, Bambina S, Berman A, Cherry S.** 2009. Autophagy is an essential component of Drosophila immunity against vesicular stomatitis virus. Immunity **30:**588–598. http://dx.doi.org/10.1016/j.immuni.2009.02.009.
51. **Lee HK, Lund JM, Ramanathan B, Mizushima N, Iwasaki A.** 2007. Autophagy-dependent viral recognition by plasmacytoid dendritic cells. Science **315:**1398–1401. http://dx.doi.org/10.1126/science.1136880.
52. **Tallóczy Z, Virgin HW, Levine B.** 2006. PKR-dependent autophagic degradation of herpes simplex virus type 1. Autophagy **2:**24–29. http://dx.doi.org/10.4161/auto.2176.
53. **Lee YR, Lei HY, Liu MT, Wang JR, Chen SH, Jiang-Shieh YF, Lin YS, Yeh TM, Liu CC, Liu HS.** 2008. Autophagic machinery activated by dengue virus enhances virus replication. Virology **374:**240–248. http://dx.doi.org/10.1016/j.virol.2008.02.016.
54. **Heaton NS, Randall G.** 2011. Dengue virus and autophagy. Viruses **3:**1332–1341. http://dx.doi.org/10.3390/v3081332.
55. **Krejbich-Trotot P, Gay B, Li-Pat-Yuen G, Hoarau JJ, Jaffar-Bandjee MC, Briant L, Gasque P, Denizot M.** 2011. Chikungunya triggers an autophagic process which promotes viral replication. Virol J **8:**432. http://dx.doi.org/10.1186/1743-422X-8-432.
56. **Li JK, Liang JJ, Liao CL, Lin YL.** 2012. Autophagy is involved in the early step of Japanese encephalitis virus infection. Microbes Infect **14:**159–168. http://dx.doi.org/10.1016/j.micinf.2011.09.001.
57. **Vandergaast R, Fredericksen BL.** 2012. West Nile virus (WNV) replication is independent of autophagy in mammalian cells. PLoS One **7:**e45800. http://dx.doi.org/10.1371/journal.pone.0045800.
58. **Panyasrivanit M, Greenwood MP, Murphy D, Isidoro C, Auewarakul P, Smith DR.** 2011. Induced autophagy reduces virus output in dengue infected monocytic cells. Virology **418:**74–84. http://dx.doi.org/10.1016/j.virol.2011.07.010.
59. **Ke PY, Chen SS.** 2011. Activation of the unfolded protein response and autophagy after hepatitis C virus infection suppresses innate antiviral immunity in vitro. J Clin Invest **121:**37–56. http://dx.doi.org/10.1172/JCI41474.
60. **Dreux M, Gastaminza P, Wieland SF, Chisari FV.** 2009. The autophagy machinery is required to initiate hepatitis C virus replication. Proc Natl Acad Sci U S A **106:**14046–14051. http://dx.doi.org/10.1073/pnas.0907344106.
61. **Heaton NS, Randall G.** 2010. Dengue virus-induced autophagy regulates lipid metabolism. Cell Host Microbe **8:**422–432. http://dx.doi.org/10.1016/j.chom.2010.10.006.
62. **Grard G, Caron M, Mombo IM, Nkoghe D, Mboui Ondo S, Jiolle D, Fontenille D, Paupy C, Leroy EM.** 2014. Zika virus in Gabon (Central Africa)—2007: a new threat from Aedes albopictus? PLoS Negl Trop Dis **8:**e2681. http://dx.doi.org/10.1371/journal.pntd.0002681.
63. **Benedict MQ, Levine RS, Hawley WA, Lounibos LP.** 2007. Spread of the tiger: global risk of invasion by the mosquito Aedes albopictus. Vector Borne Zoonotic Dis **7:**76–85. http://dx.doi.org/10.1089/vbz.2006.0562.
64. **Medlock JM, Hansford KM, Schaffner F, Versteirt V, Hendrickx G, Zeller H, Van Bortel W.** 2012. A review of the invasive mosquitoes in Europe: ecology, public health risks, and control options. Vector Borne Zoonotic Dis **12:**435–447. http://dx.doi.org/10.1089/vbz.2011.0814.